AD-A137 018 AN INVESTIGATION OF NEW POSSIBILITIES TO SIMPLIFY THE STANDARD SUPERSONIC AREA RULE(U) AIR FORCE INST OF TECH WRIGHT-PATTERSON AFB OH SCHOOL OF ENGI.. V R NIKOLIC

UNCLASSIFIED DEC 83 AFIT/GAE/AA/83D-16 F/G 20/4 NL

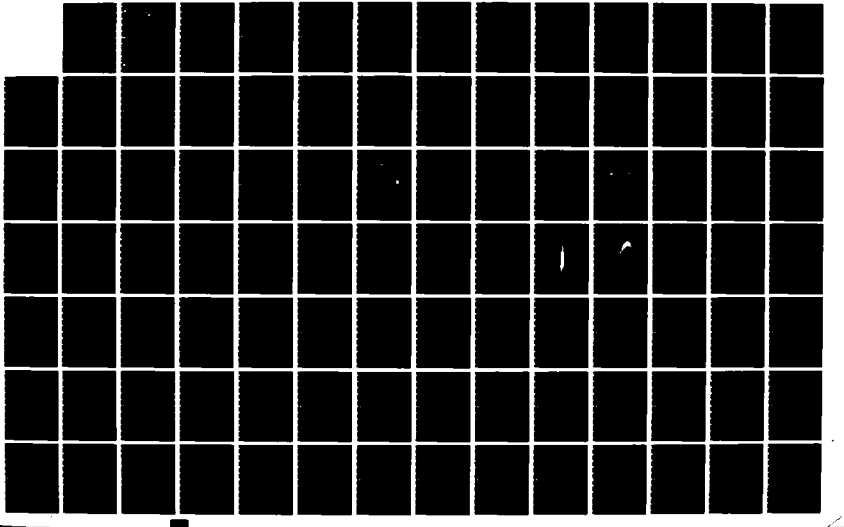

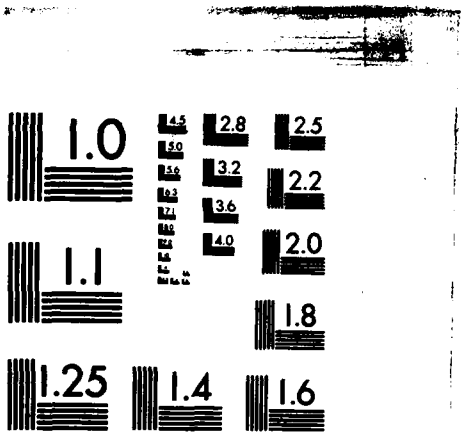

AD A137018

AN INVESTIGATION OF NEW POSSIBILITIES TO SIMPLIFY THE STANDARD SUPERSONIC AREA RULE

THESIS

AFIT/GAE/AA/83D-16

Vojin Rade Nikolic
Capt, First Class YAF

DTIC FILE COPY

DEPARTMENT OF THE AIR FORCE
AIR UNIVERSITY
AIR FORCE INSTITUTE OF TECHNOLOGY

Wright-Patterson Air Force Base, Ohio

84 01 17 076

AFIT/GAE/AA/83D-16

AN INVESTIGATION OF NEW POSSIBILITIES TO SIMPLIFY THE STANDARD SUPERSONIC AREA RULE

THESIS

AFIT/GAE/AA/83D-16 Vojin Rade Nikolic
Capt. First Class YAF

AFIT/GAE/AA/83D-16

AN INVESTIGATION OF NEW POSSIBILITIES TO SIMPLIFY THE STANDARD SUPERSONIC AREA RULE

THESIS

Presented to the Faculty of the School of Engineering

of the Air Force Institute of Technology

Air University

In Partial Fulfillment of the

Requirements for the Degree of

Master of Science

by

Vojin Rade Nikolic

Captain First Class YAF

Graduate Aeronautical Engineering

December 1983

Preface

This study attempted to simplify the supersonic area rule. I achieved promising results.

I would like to thank my thesis advisor, Major (Dr.) Eric Jumper for his assistance and guidance. I would also like to acknowledge the help I received from my committee members, Dr. Peter Torvik and Lt. Col. (Dr.) Michael Smith. Finally, a special note of gratitude to my wife, Danica, and our two sons, Zlatko and Vladan, for their sacrifices and support.

Vojin R. Nikolic

Table of Contents

	Page
Preface	ii
List of Figures	iv
List of Tables	vi
Abstract	vii
I. Introduction	1
II. The Supersonic Area Rule - Review of the Basic Theory and Previous Attempts to Simplify the Method	4
Supersonic Drag	4
Mechanism of the Wave Drag Creation	5
Lomax's Result for the Wave Drag Coefficient	8
Jones' Result -- The Supersonic Area Rule	19
Use of the Supersonic Area Rule	22
Simplifications to the Supersonic Area Rule	27
Four New Proposed Simplifications of the Supersonic Area Rule	35
III. Results and Discussion	39
F-15 With and Without the Conformal Pallet T-94	40
F-105 With and Without the Rear Body Bump	47
Northrop F-5E (Single Seat) and the F-5F (Two Seat) Versions	51
Two V/STOL Airplane Configurations With Wings of Variable Sweep	59
Two Aircraft Configurations Designed for Different Mach Numbers	62
Two Delta Wing-Body Combinations Contoured as Specified by the Transonic Area Rule	63
The Effect of the Canopy Location on the Wave Drag of a Sweptback Wing-Body Configuration	65
Sensitivity of the Results to the Input Data Accuracy	67
IV. Theoretical Reasoning for the Results Obtained	71
V. Conclusions	73
Bibliography	74
Appendix I. Description of the Computer Programs Written to Incorporate New Simplifications	77
Vita	90

List of Figures

Figure		Page
1	Momentum Control Surface for Drag Calculation	7
2	Composition of Drag for Delta-Wing Design in Level Flight	7
3	Areas in Oblique Planes	10
4	Forces in Oblique Planes	16
5	Use of the Supersonic Area Rule	24
6	Area Distribution Given by Intersection of Mach Planes .	28
7	Drag of Complete Configuration and Equivalent Bodies . .	30
8	Jumper's Modification	31
9	Comparison of Predicted Wave Drag at Zero-Lift	34
10	Four Versions of the New Proposed Simplification	37
11	Location of the T-94 Pallet	41
12	Area Distribution of the F-15 With and Without the Fast Pack Pallets Attached	42
13	Incremental Drag Due to Adding the Fast Pack Fuel Pallets	43
14	Predicted Zero-Lift Wave Drag of the F-15 Clean	44
15	Predicted Zero-Lift Wave Drag of the F-15 with the T-94 Pallets	45
16	Incremental Drag Due to Adding the Pallets	46
17	The F-105 REPUBLIC With and Without the Rear-Body Bump .	48
18	Some Predicted and Measured Drag Data of the F-105 Without the Rear Body Bump	49
19	Some Predicted and Measured Drag Data of the F-105 Aircraft With the Rear Body Bump	50
20	Predicted Zero-Lift Wave Drag of the F-5E Aircraft . . .	54

Figure		Page
21	Comparison of Zero-Lift Wave Drag	55
22	Relative Errors in Zero-Lift Wave Drag Data for the F-5E Aircraft	56
23	Comparison of Zero-Lift Wave Drag Data for the F-5F Aircraft	58
24	Two Generic Aircraft Configurations	64
25	The Input Data Error Effects: (a) Jumper's Method and (b) Version II'	69
26	Flow Chart of the New Proposed Simplifications	78
27	Binary Search Procedure	82

List of Tables

Table		Page
I	F-105 With and Without the Rear Body Bump (Zero-Lift Wave Drag Comparison)	52
II	Zero-Lift Wave Drag Coefficient of the F-5F Aircraft . .	57
III	Wave Drag Characteristics of Two V/STOL Aircraft	60
IV	Zero-Lift Drag Differences for Two Generic Aircraft . . .	64
V	The Effect of the Canopy Location on Zero-Lift Drag of a Sweptback Wing Body Combination	66
VI	Sensitivity of the Results to the Input Data Accuracy . .	68

Abstract

An investigation was conducted to find out whether there are possibilities to construct a procedure capable of giving reasonably accurate results for the aircraft wave drag coefficient over a range of Mach numbers or, at least, to predict the wave drag changes due to configuration changes.

The idea was to build an algorithm starting from the standard supersonic area rule but employing different definitions for the area distribution along the longitudinal axis as applied to the equivalent body of revolution. Instead of using the set of planes tangent to the characteristic Mach cones, lateral surfaces of the cones were used. A computer program to perform the calculations following the procedure proposed was written.

Several aircraft configurations were investigated by employing the developed method and very promising results for a particular type of supersonic aircraft configuration at moderate supersonic speeds have been obtained. When applied to predict the wave drag of a configuration employing a thin wing of small aspect ratio centrally mounted on a slender fuselage at Mach numbers between 1.4 and 2.0, the method gave results within a range of ten percent accuracy.

AN INVESTIGATION OF NEW POSSIBILITIES TO SIMPLIFY THE STANDARD SUPERSONIC AREA RULE

I. Introduction

Since its appearance the supersonic area rule has been extensively used as a powerful tool for predicting the aircraft wave drag coefficient. Jones' result, known as the supersonic area rule, has proven itself as a good approximation to the correct linearized theory result, the one given by Lomax. The degree of approximation has particularly been very high for such cases as non-lifting wings centrally mounted on slender body type fuselages.

Several computer programs employing the supersonic area rule have been written. The one written by Boeing Company (Ref 1) in the 1960's has been widely used both as a complete program for the wave drag calculations or as a part of more complex programs for the airplane design purposes. This is by no means the only program in use today; the 124J Program (Ref 2) has been developed by Northrop Company, the Langley Research Center (Ref 2) has written another program, and so forth. What all of these programs have had in common is significant complexity of the input data set required and large core requirements (Ref 3) which means that without access to large computer systems one cannot even think of employing the procedure. This has been the reason for aerodynamicists along the way to try to simplify somewhat the method. Several such attempts are described in Section II, and particularly one done by E. J. Jumper (Ref 3).

The purpose of the study described in this paper was to investigate the possibility of modifying the supersonic area rule in the following way. Rather than using families of parallel planes always tangent to the characteristic Mach cones, the lateral surfaces of the cones themselves are employed. This, together with approximating an airplane by an equivalent body of revolution, represents the essence of the modification proposed (Ref 4). Obviously, several possibilities of defining the ar of interest at a given axial location exist, i.e., either the forward or backward Mach cone can be used, and each of the two choices can be divided further into two sub-cases so that four different definitions for S(x) can be defined and algorithms for each of the cases were devised and incorporated into a computer program (i.e., four versions of the same program). Aircraft configurations for which data exist were used to determine the validity of each of the four methods. The version employing the backward projection of the down-stream Mach cone proved superior over the others.

Along with the portion of the study described above, this study has been a kind of further numerical validation of the procedure proposed by E. J. Jumper (Ref 3). His method gave good results, particularly at transonic and lower supersonic Mach numbers and proved generally superior to the four proposed new methods.

The advantages of all these methods over use of the full supersonic area rule are that they require very simple input format and the programs can be run on almost any computer with only modest core.

The present study has pointed out that the two methods, the Jumper method and the method developed by making use of the down-stream Mach cone

cut area projection, should be investigated further both analytically and numerically by applying them to a number of systematically chosen aircraft configurations. It would be rather important to have at hand a relatively simple method capable of giving quick results within limits of, say, ten percent accuracy. Such a method would be useful for early project management decisions and design studies. The fact that high speed computers of enormous capabilities and modern aerodynamic design methods are readily available does not eliminate the need for simple procedures easily prepared and performed.

II. The Supersonic Area Rule - Review of the Basic Theory and Previous Attempts to Simplify the Method

Supersonic Drag

If one assumes that the flow is nowhere separated, the drag of an aircraft flying at supersonic speeds is due to the following three mechanisms:

1. Skin friction drag
2. Vortex drag
3. Wave drag

The first two drag components are essentially the same as in subsonic flow. The third component -- the wave drag -- represents a peculiarity of supersonic flows and will be treated in more detail.

Skin friction drag is due to the phenomena that occur in boundary layers -- thin layers of viscous fluid near to the aircraft surface. To determine this drag component an aerodynamicist should perform calculation of the boundary layer in a manner basically the same as for subsonic flow. It should be pointed out that this component may represent a considerable fraction of the total aircraft drag (a typical amount is 30 percent). So, any realistic drag analysis must include the skin friction drag.

The vortex drag arises from the momentum, and hence kinetic energy left in the fluid as a lifting vehicle, travels through it (Ref 5). Since the vorticity remains essentially stationary with the fluid, there is no fundamental difference between this drag at subsonic and supersonic speeds. In fact, the vortex drag can be calculated by use of formula for the induced drag of a lifting three-dimensional wing in incompressible flow. In the supersonic case, however, the lift will induce an additional

drag component, namely the wave drag due to lift.

Mechanism of the Wave Drag Creation

The wave drag is an aerodynamic phenomenon unique to supersonic flow and is associated with the energy radiated away from the vehicle in the form of pressure waves in much the same way as a fast-moving ship causes waves on the water surface (Ref 5).

The wave drag of a planar wing can be divided into two parts: the wave drag due to thickness and the wave drag due to lift. Often the sum of the wave drag and the vortex drag is called the pressure drag since it is manifested by the pressure times the chord-wise slope of the wing or body surface.

As stated in Reference 6, in a steady inviscid subsonic flow, the pressure drag arising from the thickness of the body or wings is negligible so long as the shapes are sufficiently well streamlined to avoid flow separation. In that case there exists no possibility of either favorable or adverse interference on the pressure distributions themselves. If one body is so placed as to receive a drag from another, then the second body is sure to receive a corresponding increment of thrust from the first.

At supersonic speeds this tolerance disappears and drag becomes sensitive to the shape and arrangement of the bodies. While it appears that the primary factor here is the thickness ratio (Ref 7), there exist arrangements in which a large cancellation of drag occurs. Examples of the latter are the sweptback wing and the Busemann biplane.

Whitcomb has found that the major part of the supersonic wave drag for a wing-body combination results from losses associated with shocks

at considerable distances from the configuration (Ref 8). This led him to the conclusion that the wave drag may be estimated by considering the stream disturbances produced by a configuration at these distances.

Leyman and Markham stated that on physical grounds wave drag is most satisfactorily associated with the entrophy rise across the shock waves, but this is not very useful in practice (Ref 9). Within the linearized theory one can calculate wave drag by considering the lateral convection of streamwise momentum. The distinction between wave drag and vortex drag becomes clearer when we attempt to calculate the drag from momentum considerations. For this purpose we surround the vehicle by a control surface consisting of a cylindrical surface, S_2, of radius R closed by two end planes, S_1 and S_3 (see Figure 1). For present purposes, we assume that the radius R is very large compared with a typical dimension of the aircraft. We also assume S_1 and S_3, the end surfaces, to be placed well away from the vehicle which in turn is assumed to have negligible base areas. A consideration of the momentum flow through the surfaces gives, to lowest order, the stream-wise force component

$$\frac{D}{q} = -2 \iint_{S_2} \Phi_x \Phi_r \, dS_2 + \iint_{S_3} (\Phi_y^2 + \Phi_z^2) \, dS_3 \qquad (1)$$

where $q = (1/2)\rho U^2$, and x, y, z are the wind axes.

The first term represents the wave drag, which in the absence of any trailing vorticity will be equal to the pressure drag. The second term represents the vortex drag of the vehicle which is identical to

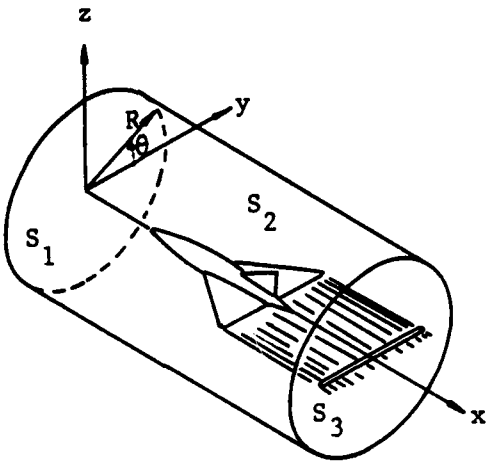

Figure 1. Momentum Control Surface for Drag Calculation

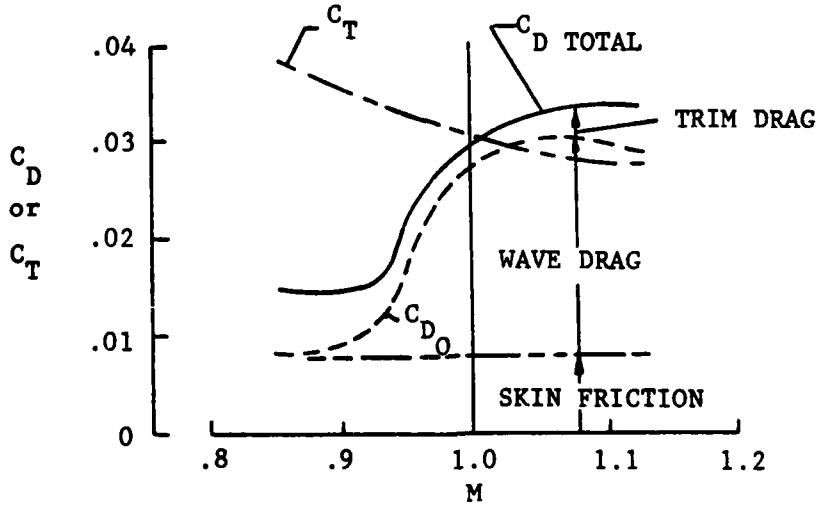

Figure 2. Composition of Drag for Delta-Wing Design In Level Flight

the induced drag for subsonic flow. Here, Φ is the perturbation velocity potential and Φ_x, Φ_y, and Φ_r are the perturbation velocity components.

The wave drag component amounts to a considerable fraction of the total aircraft drag. Donlan pointed out that the wave drag can create formidable design problems as illustrated in Figure 2 (Ref 10). For the flight condition assumed, the drag coefficient associated with level flight increases markedly with Mach number as the speed of sound is approached and exceeded. While the friction component and the trim drag component (including induced drag) are still of significance at supersonic speeds, the wave drag component is responsible for the large increase in drag coefficient shown. The wave drag component is primarily independent of the lift and thus can usually be analyzed for the zero-lift condition.

Lomax's Result for the Wave Drag Coefficient

Lomax (Ref 11) presented the development of an exact (within framework of the linearized theory) formula for the wave drag of any lifting or non-lifting object in a steady supersonic flow. He considered a supersonic flow subject to the following assumptions:

-- Steady flow
-- Small angle of attack

Then the disturbed flow field may be approximated by the following linearized potential flow equation:

$$\beta^2 \phi_{xx} - \phi_{yy} - \phi_{zz} = 0 \qquad (2)$$

where the free-stream is moving in the positive x direction and $\beta^2 = M_\infty^2 - 1$.

Lomax made use of the general solution to Eq (2) given by Volterra:

$$\phi(x,y,z) = -\frac{1}{2\pi}\frac{\partial}{\partial x}\iint_{\tau}\left(\frac{\partial\phi}{\partial\nu_1} - \phi\frac{\partial}{\partial\nu_1}\right)\ln\frac{x-x_1+\sqrt{(x-x_1)^2-\beta^2 r_1^2}}{\beta r_1}\,dS_1 \quad (3)$$

where $r_1^2 = (y-y_1)^2 + (z-z_1)^2$, and dS_1 is an element of surface area on the airplane, ν_1 is the outward conormal (the conormal to the characteristic cone lies along the cone) to that element, and τ is that portion of the airplane surface within the Mach cone from the point x,y,z.

The wave drag of the airplane can be expressed in terms of the perturbation velocities induced by the object on an enclosing cylindrical control surface of infinite radius. The equation employed for that purpose is conveniently written in terms of the cylindrical coordinate system defined in Figure 3a. It should be pointed out that the control surface is parallel to the free-stream direction, that is, the relative wind defines the x coordinate. Then the wave drag is given by

$$D = -\rho_\infty\int_0^{2\pi} d\theta\int_{-\infty}^{\infty} dx\,\left(\lim_{r\to\infty}\phi_r\,\phi_x\right) \quad (4)$$

Under the assumptions at the beginning of this section the wave drag of an arbitrary body is calculated by using Eq (3) to find the two derivatives needed for Eq (4). Eq (3), however, requires the conormal

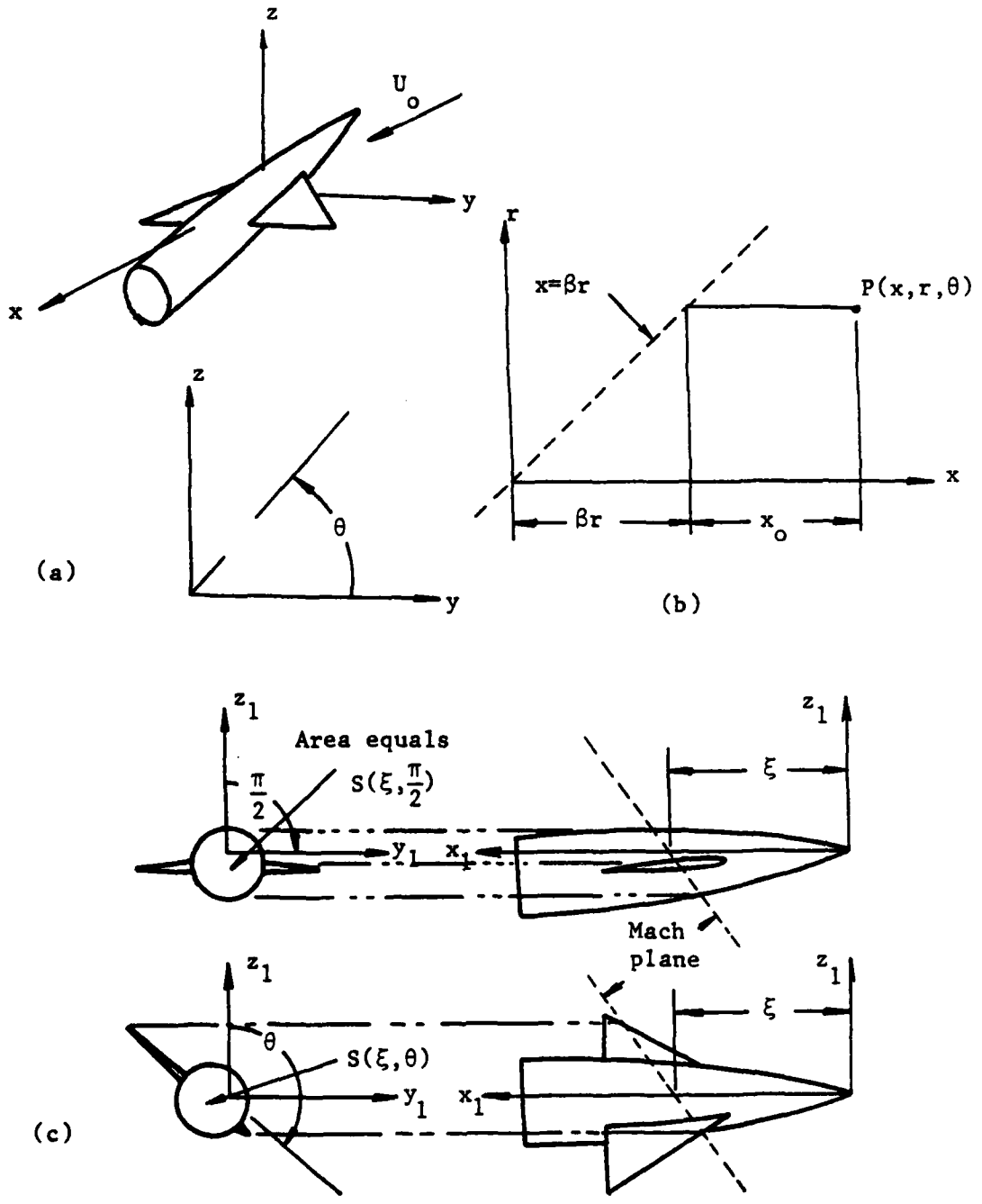

Figure 3. Areas in Oblique Planes

partial derivative ($\frac{\partial}{\partial \nu_1}$) and the differential element (dS_1). Within the framework of linearized theory these are given by

$$\frac{\partial}{\partial \nu_1} = \frac{\partial}{\partial n_1} \tag{5}$$

and

$$dS_1 = ds_1 \, dx_1 \tag{6}$$

where n_1 is either the normal to the airplane surface or the normal to the surface in the y_1, z_1 plane, and ds_1 is an element of arc along the airplane surface in an x_1 = constant plane.

The perturbation potential given by Eq (3) is now, for convenience, divided into two parts:

$$\phi(x,y,z) = \phi_1(x,y,z) + \phi_2(x,y,z) \tag{7}$$

The two terms in Eq (7) are given as:

$$\phi_1(x,y,z) = -\frac{1}{2\pi} \frac{\partial}{\partial x} \int\int_{\tau} \phi n_1(x_1,s_1) \ln \frac{x-x_1 + \sqrt{(x-x_1)^2 - \beta^2 r_1^2}}{\beta r_1} \, dx_1 \, ds_1 \tag{8}$$

and

$$\phi_2(x,y,z) = \frac{1}{2\pi}\frac{\partial}{\partial x}\int\int_{\tau}\phi(x_1,s_1)\frac{\partial}{\partial n_1}\ln\frac{x-x_1+\sqrt{(x-x_1)^2-\beta^2 r_1^2}}{\beta r_1}\,dx_1\,ds_1 \qquad (9)$$

and each of the two terms can be considered separately, i.e., the partials ϕ_x and ϕ_r of both parts are needed for Eq (4). Further, the partials are to be found in the limit as $r = \sqrt{y^2 + Z^2}$ goes to infinity. However, since no disturbance can be induced ahead of the foremost Mach cone enveloping the disturbing object, it is convenient to increase x as r is increased so that the point (x,r,θ) remains in the vicinity of this Mach cone (Ref 11:5). After setting $x = x_o + \beta r$ (Figure 3b), as r becomes very large, one can show that Eq (8) reduced to

$$\phi_1(x,r,\theta) = \frac{-1}{2\pi\ 2\beta r}\int\int_{\tau}\frac{\phi n_1(x_1,s_1)\,dx_1\,ds_1}{\sqrt{x_o - x_1+\beta y_1\ \mathrm{Cos}\ \theta + \beta Z_1\ \mathrm{Sin}\ \theta}} \qquad (10)$$

If we now introduce the following transformation

$$\xi = x_1 - \beta y_1\ \mathrm{Cos}\ \theta - \beta Z_1\ \mathrm{Sin}\ \theta$$

$$\sigma = S_1 \qquad (11)$$

Eq (10) is further simplified to

$$\phi_1(x,r,\theta) = -\frac{1}{2\pi\sqrt{2\beta r}} \int_{-\infty}^{x_o} \frac{d\xi}{x_o - \xi} \int_{oc} \phi n_1 \left| \xi - f(\xi,\sigma),\ \sigma \right| d\sigma \qquad (12)$$

where $\int_{oc} d\sigma$ is a line integral around the airplane surface in the oblique cut.

The velocity potential ϕ_1 given by Eq (12) is exactly the same as that induced on a large cylinder by a line of sources distributed along the x_1 - axis from $-\infty$ to x_o, the variation of their strength given by $\phi n_1 d\sigma$. This was first pointed out by Hayes (Ref 12).
oc

The physical meaning of the term $\int_{oc} \phi n_1 d\sigma$ can be more easily understood with aid of Figure 3c (Ref 11:7). Imagine a series of Mach planes parallel to the y_1 - axis each given by the equation $x_1 - \beta Z_1 =$ constant. Place the airplane in its normal flight attitude. Each Mach plane slices through the airplane, defining, thereby, a certain area composed of the region on the Mach plane within the airplane surface. Project these areas on planes normal to the free-stream (i.e., y_1, Z_1 planes) and designate the resulting area distribution by $S(\xi,\frac{\pi}{2})$. The integral $\int_{oc} \phi n_1 d\sigma$ is then proportional to the stream-wise rate of change of these normally projected, obliquely cut areas; that is, for the airplane so placed,

$$\int_{oc} \phi n_1 d\sigma = U_o \frac{\partial}{\partial \xi} S(\xi,\tfrac{\pi}{2})$$

Now, keeping the Mach planes fixed, revolve the airplane about the

x_1 - axis (not about its own body axis unless the latter happens to coincide with the x_1 - axis). The same effect would be achieved by holding the airplane fixed and rotating the Mach planes always tangent to the characteristic Mach cones. Now, repeat the above process for all orientations, θ, in a complete 360-degree rotation. For any given angle

$$\int_{oc} \phi n_1 d\sigma = U_o \frac{\partial}{\partial \xi} S(\xi,\theta) = U_o S'(\xi,\theta) \tag{13}$$

Since it can be shown that $(\phi_r)_{r\to\infty} = -\beta(\phi_x)_{r\to\infty}$ combining Eqs (12) and (13) gives

$$(\phi_{1x})_{r\to\infty} = -\frac{1}{\beta}(\phi_{1r})_{r\to\infty} = \frac{U_o}{2\pi\sqrt{2\beta r}} \int_{-\infty}^{x_o} \frac{S''(\xi,\theta)\, d\xi}{\sqrt{x_o - \xi}} \tag{14}$$

which, by means of Eq (4), gives the complete contribution to the wave drag of the first term in Eq (3).

But, according to Eq (7) there is one more term to be accounted for -- that one given by Eq 9. Taking the derivative with respect to n_1, then proceeding as before, setting

$$x = x_o + \beta r ,$$

$$y = r \text{ Cos } \theta ,$$

$$z = r \text{ Sin } \theta$$

and letting r go to infinity and employing the transformation given by Eq (11), ϕ_2 can be expressed as

$$\phi_2(x,r,\theta) = \frac{\beta}{2\pi\sqrt{2\beta r}} \frac{\partial}{\partial x_o} \int_{-\infty}^{x_o} \frac{d\xi}{\sqrt{x_o - \xi}} \int_{oc} \phi\left[\xi - f(\xi,\sigma),\sigma\right] \times \left(\frac{dy_1}{dn_1} \text{Cos } \theta + \frac{dZ_1}{dn_1} \text{Sin } \theta\right) d\sigma \quad (15)$$

The nomenclature is given in Figure 4a (Ref 11:9) from where we can notice that the term

$$\left(\frac{dy_1}{dn_1} \text{Cos } \theta + \frac{dZ_1}{dn_1} \text{Sin } \theta\right) ds_1$$

is simply the component of ds_1 normal to the constant - θ plane. If we designate this direction by the coordinate σ_θ, as in Figure 4a, Eq (15) becomes

$$\phi_2(x,r,\theta) = \frac{\beta}{2\pi\sqrt{2\beta r}} \frac{\partial}{\partial x_o} \int_{-\infty}^{x} \frac{d\xi}{\sqrt{x_o - \xi}} \int_{oc} \phi d\sigma_\theta$$

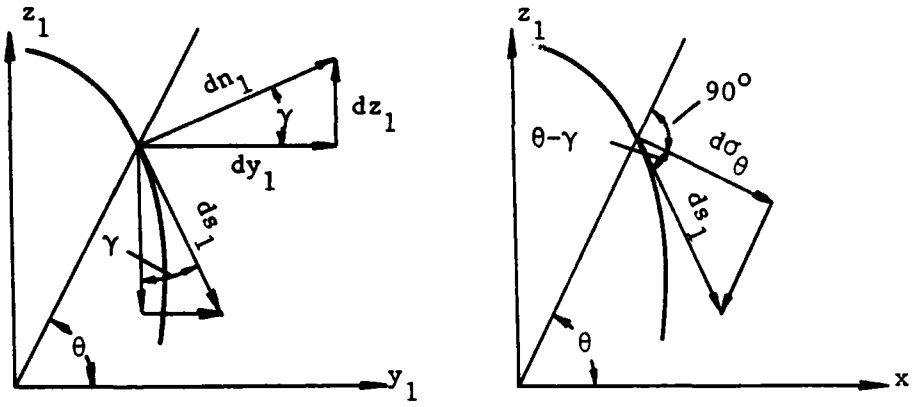

$$\frac{dy_1}{dn_1} = \cos\gamma \; ; \; \frac{dz_1}{dn_1} = \sin\gamma$$

$$\cos\gamma\cos\theta + \sin\gamma\sin\theta = \cos(\gamma-\theta)$$

(a)

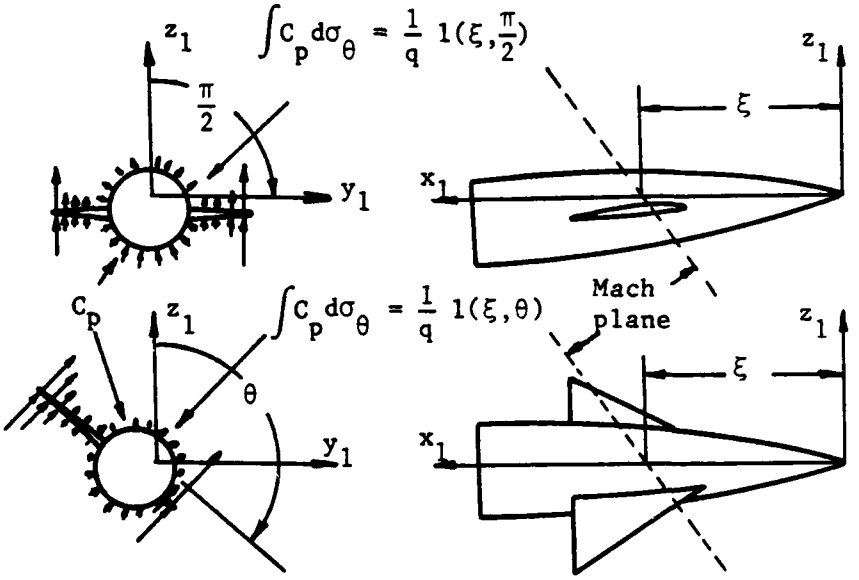

(b)

Figure 4. Forces in Oblique Planes

Further, notice that

$$\frac{\partial}{\partial \xi} \phi \left[\xi - f(\xi,\sigma)\sigma \right] = U \left[\xi - f(\xi,\sigma)\sigma \right]$$

where $U(x,\sigma) = \frac{\partial}{\partial x} \phi(x,\sigma)$, since in linearized theory partial $\frac{\partial f}{\partial \xi}$ is considered small relative to unity. If the relation for pressure coefficient is introduced,

$$C_p = \frac{p - p_o}{\frac{1}{2} \rho_o U_o^2} = - \frac{2\phi_x}{U_0} \tag{16}$$

the result of integrating by parts yields

$$\phi_2(x,r,\theta) = \frac{-\beta U_o}{4\pi\sqrt{2\beta r}} \int_{-\infty}^{x_o} \frac{d\xi}{\sqrt{x_o - \xi}} \int_{oc} C_p d\sigma_\theta \tag{17}$$

This velocity potential is again exactly the same as that induced on a large cylinder by a line of sources distributed along the x_1 - axis from $-\infty$ to x_o, the variation of their strength this time being given by $\frac{\beta U_o}{2} \int_{oc} C_p d\sigma_\theta$ (Ref 11:9). The physical significance of $\int_{oc} C_p d\sigma_\theta$ can be demonstrated with the aid of Figure 4b (Ref 11:10). Once again let us

imagine a series of planes described by equation $s_1 - \beta Z_1 = \text{const}$, parallel to the y_1 - axis. With the airplane placed in its normal flight attitude, $l(\xi,\frac{\pi}{2})$ is defined as the lift (the component of net resultant force in the Z_1 direction, positive upward) on a given section formed by the intersection of a Mach plane with the airplane surface. It can be shown that the integral is

$$\int_{oc} C_p d\sigma_\theta = \frac{1}{q} l\ (\xi,\frac{\pi}{2})$$

where q is the free-stream dynamic pressure. With the coordinate system fixed and the airplane rotated about the x_1 - axis, at each new θ angle, the term $q \int_{oc} C_p d\sigma_\theta$ represents the net lift on the oblique cut at that particular x_1, i.e.,

$$\int_{oc} C_p d\sigma_\theta = \frac{1}{q} l\ (\xi,\theta) \qquad (18)$$

If, on the other hand, the airplane is fixed and the Mach planes are rotated, $l(\xi,\theta)$ represents the resultant obliquely cut section force normal to the free-stream and parallel to the plane given by θ = constant.

Plugging Eq (18) into (17) we obtain

$$(\phi_{2x})_{r\to\infty} = -\frac{1}{\beta}(\phi_{2r})_{r\to\infty} = \frac{U_o}{2\pi\sqrt{2\beta r}} \int_{-\infty}^{x_o} \frac{\frac{\beta}{2q}\, l'(\xi,\theta)d\xi}{\sqrt{x_o - \xi}} \qquad (19)$$

where $l'(\xi,\theta) = \frac{\partial}{\partial\xi}\, l(\xi,\theta)$ is the stream-wise gradient of the "lift" on the obliquely cut section. After placing Eqs (14) and (19) into Eq (4) and carrying out the x integration the following result is obtained:

$$\frac{D}{2} = -\frac{1}{4\pi^2} \int_o^{2\pi} d\theta \int_{-L_1(\theta)}^{L(\theta)} dx_1 \int_{-L_1(\theta)}^{L(\theta)} dx_2 \left[S''(x_1,\theta) - \frac{\beta}{2q}\, l'(x_1,\theta) \right]$$

$$\times \left[S''(x_2,\theta) - \frac{\beta}{2q}\, l'(x_2,\theta) \right] \ln \left| x_2 - x_1 \right| \qquad (20)$$

where for any roll angle θ = constant, the intersecting Mach planes are extended from $x = -L_1(\theta)$ to $x = L(\theta)$.

Eq (20) gives the wave drag of any lifting or non-lifting airplane in a steady supersonic flow, the only approximations being those basic to linearized theory (Ref 11).

Jones' Result -- The Supersonic Area Rule

Eq (20) given in the previous section gives the wave drag of any system of bodies or wings and bodies. The equation is subject to the usual limitations of the linearized theory.

Two different types of terms can be recognized by looking at that equation:

-- The terms containing the second derivative of $S(x,\theta)$, the so-called "area terms", and

-- The terms containing the first derivative of $l(x,\theta)$, the so-call "lift terms".

Physical meaning of both kinds was discussed in the previous section.

If we restrict Eq (20) to the case of non-lifting aircraft, the lift terms disappear from the equation. So, by neglecting the lift terms, Lomax's result reduces to the supersonic area rule formula given by Jones (Ref 6):

$$D(\theta) = -\frac{\rho U^2}{4\pi} \int_{-x_o}^{+x_o} \int_{-x_0}^{+x_o} S''(x,\theta)\, S''(x_1,\theta) \log \left| x - x_1 \right| dx dx_1 \qquad (21)$$

or, at transonic speeds

$$D_{M\to 1} = -\frac{\rho U^2}{4\pi} \int_{-x_o}^{+x_o} \int_{-x_o}^{+x_o} S''(x)\, S''(x_1) \log \left| x - x_1 \right| dx dx_1 \qquad (22)$$

Here, the limits of integration $-x_o$ and $+x_o$ correspond to $-L_1$ and L in Eq (20). The last formula states that at transonic speeds the wave drag of a wing-body combination depends solely on the longitudinal development of the total cross-sectional area intercepted by a plane perpendicular to the stream at the station x.

R. T. Whitcomb has come to the same result (Ref 13). He has shown how the drag at transonic speeds may be reduced to a surprising extent by simply cutting out a portion of the fuselage to compensate for the area blocked by the wing. This transonic aircraft design procedure was named the transonic area rule. That is the reason why Eq (21) was christened the "supersonic area rule" -- the equation being a generalization of more specific Whitcomb's result.

Whitcomb's deduction of the "area rule" was based on considerations of stream-tube area and the phenomenon of "chocking" -- which follow from one-dimensional-flow theory. Each individual stream-tube of a three-dimensional-flow field must obey the law of one-dimensional flow. While we cannot actually determine the three-dimensional field on this basis alone, nevertheless it provides a good starting point for our thinking (Ref 6).

The fact that the wave drag of wings and bodies can be related to the longitudinal area distribution of the system as a whole was first recognized by W. D. Hayes in his 1946 thesis (Ref 12). The two are related in the following manner: It is well known that the flow field about any system of bodies may be created by a certain distribution of sources and sinks over the surfaces of the bodies. Hayes' formula and some other formulas (e.g., those given by Lomax and Heaslet (Ref 14), and Spreiter (Ref 15)) relate the drag of such a system to the distribution of these singularities. To obtain a formula for the wave drag in terms of area distributions we have to adopt a simplified relation between the source strength and the geometry of the bodies, namely that the source strength is proportional to the normal component of the stream velocity

at the body surface. There are examples (e.g., Busemann biplanes and ducted bodies) for which this assumption is not valid. If, on the other hand, we limit ourselves to thin symmetrical wings mounted on vertically symmetrical fuselages, there are indications that a good estimate of the wave drag at supersonic speeds can be obtained on the basis of the simplified relation assumed (Ref 6).

It should be pointed out that only in special cases may the general theoretical formulas be reduced to the form of an area rule at both transonic and supersonic speeds. The previously mentioned pressure term (that has been neglected in arriving at both the rule concepts) represents the limiting factor to the correctness of the supersonic area rule even within the framework of linearized theory (Ref 3). Finally, it should be noted that the formula given by Eq (22) shows a striking resemblance to well-known von Karman's result for the slender body wave drag (Ref 7:239) although the restrictions on the equations are quite different.

Use of the Supersonic Area Rule

Since its appearance, the supersonic area rule has been used as a tool for calculating the wave drag of wing-body combinations. Several computer programs have been written and one of the most widely used is that developed by the Boeing Company in the 1960's described by R. V. Harris in Reference 1. The same program was included as a part of a more complex design procedure by Baals, Robins, and Harris in Reference 16, where they showed that for conventional configurations of supersonic aircraft the supersonic area rule gave good results. But it should be kept in mind that there are aircraft configurations for which the pressure

term and C_{D_L} are not small.

The following is a description of a general algorithm used to calculate the wave drag coefficient by employing the supersonic area rule method.

Let us consider the aircraft of Figure 5a. The length of the aircraft is divided into n segments, Δx in length along the aircraft longitudinal axis which for the purpose of this calculation must coincide with x_1 - axis (longitudinal axis in the wind axis system). Thus, each end point of the n segments is given by $x = i\,\Delta x$ where $i = 1,2,\ldots,n$ and $n = L/\Delta x$.

If one chooses a particular Mach number of interest, say the lowest Mach number, $M = M_1$, this defines a Mach cone having the half angle $\mu_1 = \mathrm{Sin}^{-1}(1/M_1)$, and height OV (see Figure 5b). Examining any point on the circumference of the base circle, say point A, it is easy to imagine a generator of the cone that passes through points A and V. The plane tangent to the cone at the generator VA may now be considered a "cutting tool" for determining the area cuts through the wing-body configuration. Let p be this plane. When attached to the x - axis at location $(x_1,0,0)$ such that OA is parallel to the Oz - axis, then the plane p will intersect the aircraft making a figure in p. This figure bounds the area composed of the region on the Mach plane within the airplane surface. The projected area bounded by the figure onto a plane normal to the free-stream at $x = x_1$, is the area, S_1, that we are interested in (see Figure 5c).

The cone-plane assembly is then moved along the x - axis until point V reaches point $(x_2,0,0)$, and process repeated to yield S_2 and so on until the vertex reaches point (L,0,0) supplying us with a table of values:

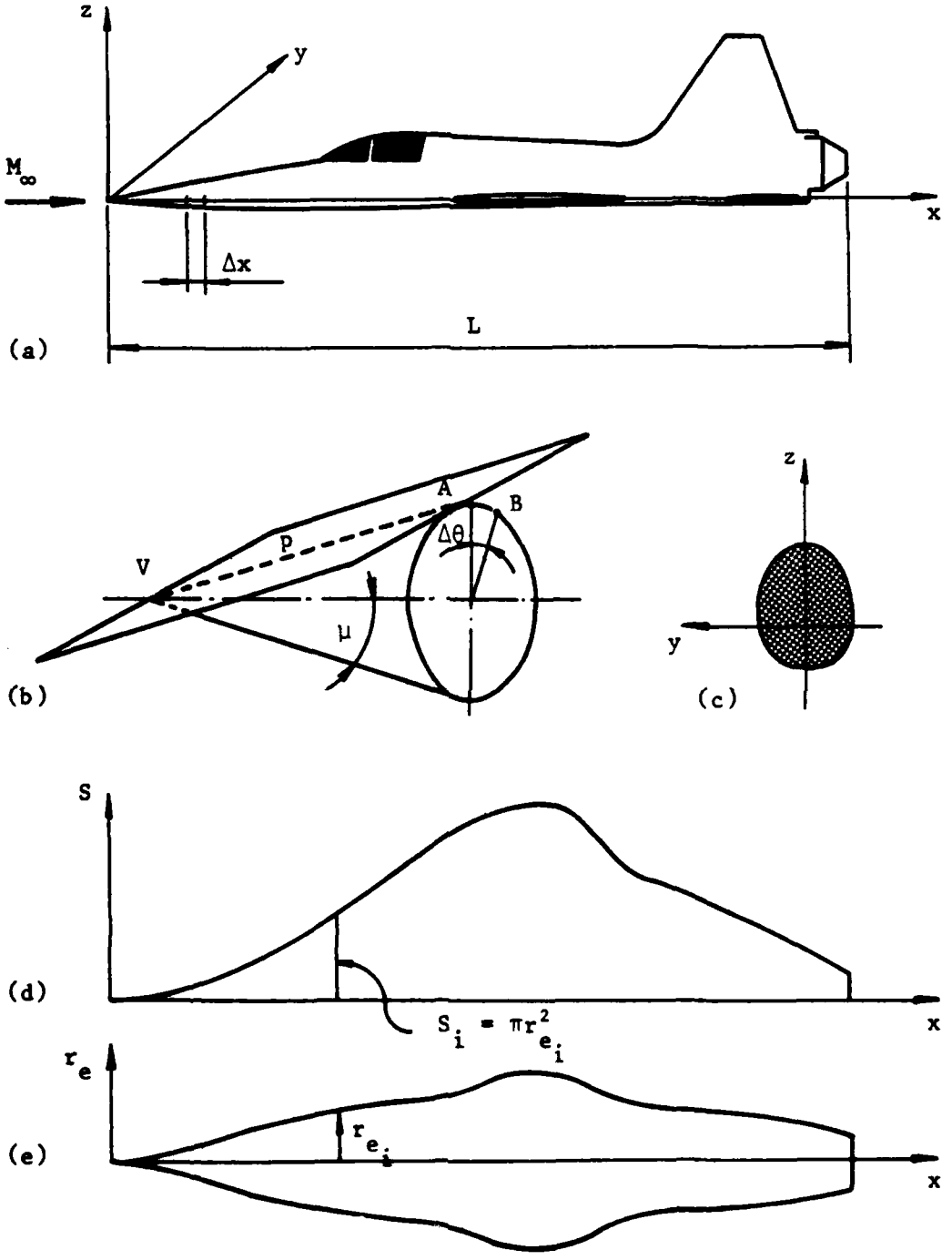

Figure 5. Use of the Supersonic Area Rule

$S_1, S_2, \ldots, S_n$ (the normal projections of the areas obtained by cutting the aircraft by Mach plane at an angle μ_1 measured from the x - axis -- see Figure 5d). This set then defines an equivalent body of revolution in the following manner:

-- The length of the body is exactly L.

-- The cross-sectional area of that body at a distance x_i from its foremost point is S_i, i = 1,2,. . .,n, (see Figure 5d).

Having the equivalent body of revolution for the single rotation angle, θ ($\theta = \frac{\pi}{2}$ for this case), Eq (21) is used to calculate the wave drag coefficient of the body of revolution at that Mach number M_1. The second derivative of S(x) needed for Eq (21) can be determined by employing a numerical scheme to first find S'(x) then S''(x). The integration required in Eq (21) is then carried out numerically.

According to Eq (20), this task must be repeated for many θ's so that the integration may be carried out numerically. This may be done by rotating the generator or taking the plane-cone assembly, "disconnecting" it and reconnecting it again along the VB generator of Figure 5b. Radii OA and OB make an angle ($\measuredangle$AOB). This angle, $\measuredangle$AOB, is the roll angle $\Delta\theta$, since the same effect could be achieved if the plane along the VA generator were fixed and the aircraft rolled about the x - axis by $\Delta\Theta$. This angle is measured from the positive y - axis, thus, the first area distribution described above corresponds to roll angle $\theta = \frac{\pi}{2}$.

The result of repeating the integration of Eq (21) gives another value for the wave drag coefficient which corresponds to $\theta = \frac{\pi}{2} - \Delta\theta$, and so on for each increment of θ through all roll angles up to 360 degrees. If the

aircraft is symmetric, these computations may stop at a θ of 180 degrees. If $\Delta\theta$ = 1 degree, a minimum of 180 such computations must be performed. In other words, 180 equivalent bodies of revolution must be constructed. The final integration of Eq (20) is just a simple average which yields the zero-lift wave drag coefficient, C_{D_0}, of the aircraft flying at that particular Mach number.

The entire process is repeated for each Mach number of interest.

Thus, in order to be applicable to analyze an aircraft configuration across the range of Mach numbers, any algorithm of this type must include three do loops:

1. Inner one over x_i, $i = 1,2,\ldots,n$
2. Medium one over θ_j, $j = 1,2,\ldots,180/\Delta\theta$
3. Outer one over M_k, $k = 1,2,\ldots,(M_{max} - M_{min})/\Delta M$

A few words should be mentioned on the cross-sectional areas obtained by cutting the complete aircraft structure by Mach planes, each of which is defined by two angles, μ and θ. It is not difficult to imagine what the cut area looks like if $\mu = 90$ (then θ has no effect). This is the limiting case for M = 1 and the supersonic area rule reduces to the transonic area rule which states that in order to obtain a low wave drag configuration we have to keep dS/dx curve as smooth as possible. Expanding S'(x) = dS/dx in a Fourier series, as Sears did, will yield a formula for the drag analogous to that one for the induced drag of a wing in terms of its span-wise load distribution. Having that, a low drag

configuration with a given base area, or with a given overall volume within the given length, may be obtained by suppressing the higher harmonics in the curve S'(x) (Ref 6).

It is more difficult to imagine the area obtained by cutting the configuration with a plane at arbitrary μ and θ. Figure 6 shows two such areas obtained by cutting an aircraft with Mach planes at different Mach angles μ and roll angles θ. The lower portion of the figure shows two longitudinal distributions. These illustrate that an optimum area distribution at one Mach number might not be an optimum distribution for another Mach number. In other words, an aircraft configuration designed (i.e., indented) for a particular Mach number may have good drag characteristics at that design Mach number (see for example Ref 6). The reason for such a phenomenon is that at higher Mach numbers, particularly above M = 1.6, the distributions become irregular, resulting in higher values of the second derivatives, $S''(x,\theta)$, and therefore, higher the wave drag coefficient values.

Simplifications to the Supersonic Area Rule

Bearing in mind the calculation complexity and the difficulty of preparing appropriate input data for the procedure described above, it is not surprising that aerodynamicists have tried to simplify the method. Harris (Ref 1) made a modification by simplifying the fuselage description. Smith, et. al. (Ref 17) described a simplification of the standard supersonic area rule that used only one set of the Mach planes -- that of parallel vertical planes which intersect the configuration planform along Mach lines (for more details, see Ref 17). They applied this exploratory

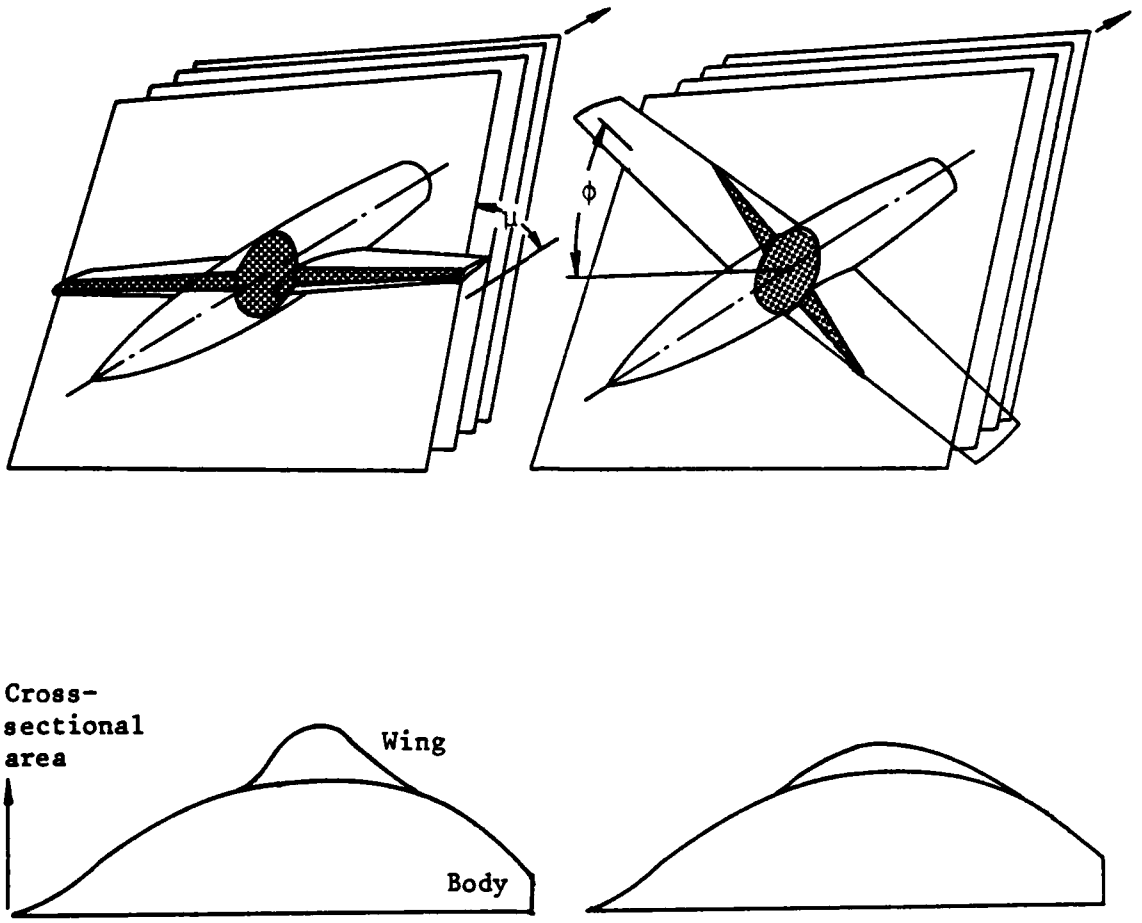

Figure 6. Area Distribution Given By Intersection of Mach Planes

approach to calculate the drag of external stores and nacelles at transonic and supersonic speeds. The data obtained showed a trend similar to that at transonic speeds. If located in a region where its area peak adds to the wing-fuselage peak (viewed along the Mach line), the store produces higher drag than if located a short distance forward or aft $x = 0$ point, x being the distance between the two peaks (Ref 12). Some of their results are shown in Figure 7.

The most fundamental simplification made to the supersonic area rule is that one proposed by Jumper (Ref 3). Jumper reduced the whole aircraft structure to a single body of revolution having the same longitudinal cross-sectional areas as the original airplane configuration. The supersonic area rule was then applied to this single body of revolution. This modification achieved two important simplifications: First, the input data set becomes the simplest possible (see Figure 8), and secondly, only one set of Mach planes need be used for each Mach number of interest. Jumper did not propose this simplified algorithm as a procedure for highly accurate wave drag predictions, but rather as an auxiliary tool for system-design studies or early program management decisions. As such, it is meant to supply the user with quick yet reasonable data, particularly if applied to predict the wave drag increment due to adding near-fuselage-axis protuberances where a good deal of information about the aircraft in question is already known.

Referring to Figure 8, instead of describing the actual aircraft configuration by inputting a large number of points in a 3-D space, Jumper proposed entering data for the normal plane cut areas along the aircraft longitudinal axis. These make up the equivalent body of revolution to

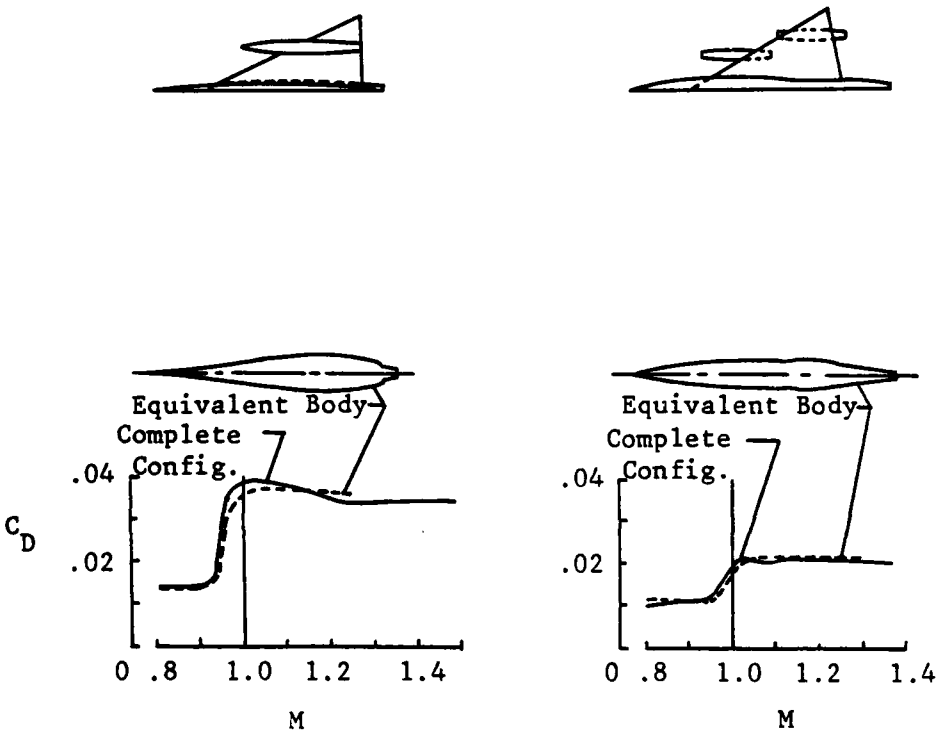

Figure 7. Drag of Complete Configuration and Equivalent Bodies

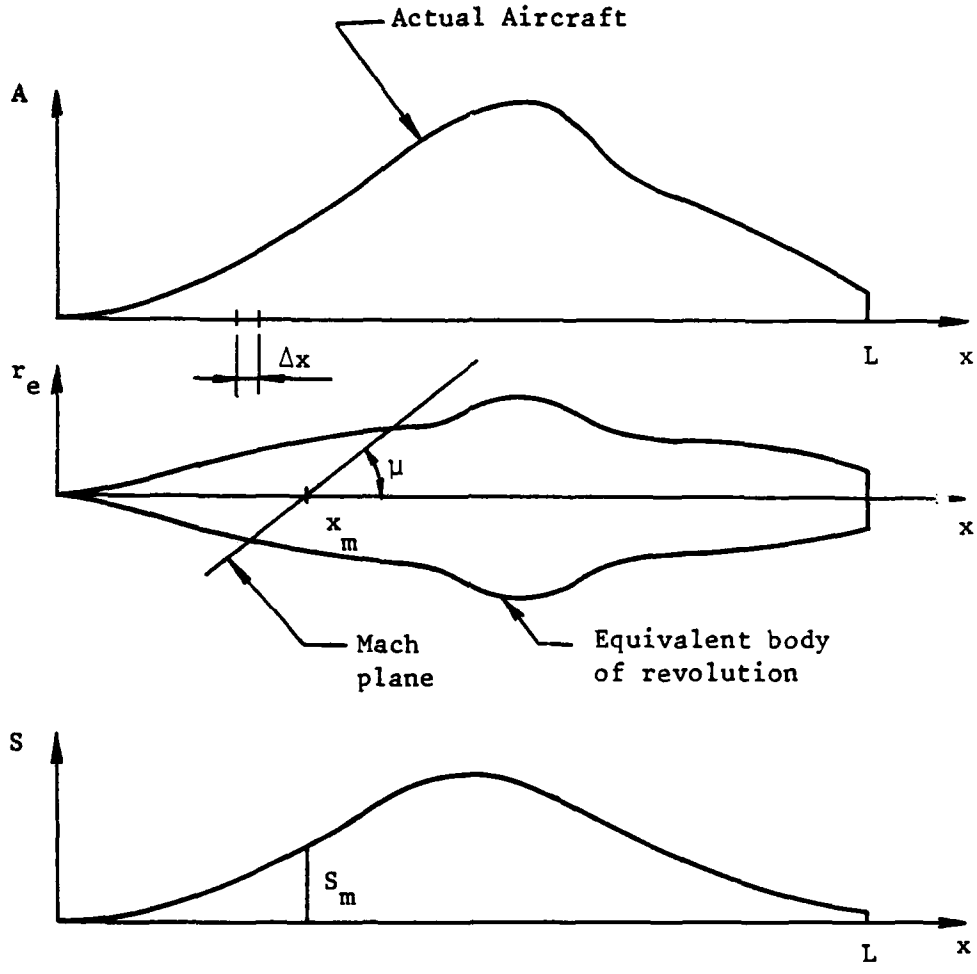

Figure 8. Jumper's Modification

which Eq (21) is applied once for each Mach number of interest -- and only once, since for a body of revolution Mach plane cut areas do not depend on a particular roll angle.

Briefly, the Jumper procedure would be as follows:

-- Enter normal planes cut areas, say $A_i = A(x_i)$.

-- Construct an equivalent body of revolution (the airplane and the body of revolution have the same cross-sectional area at any given axial location x).

-- Choose an initial Mach number which defines a Mach plane.

-- Let this Mach plane translate down-stream starting from $x_1 = \Delta x$, then $x_2 = 2\Delta x$, and so forth up to $x_n = L$.

-- At every one of these locations, take the cut area between the Mach plane and the equivalent body of revolution configuration (the linear approximation is used) and project that onto a normal plane. This will give us exactly n projected areas (S_i, $i = 1,2,\ldots,n$).

-- These projected areas define another body of revolution that has the normal plane cut area at x_i exactly equal to S_i, once again $i = 1,2,\ldots,n$.

-- Having $S_i = f(x_i)$ at a set of points we then calculate $S'(x)$ and $s''(x)$.

-- Apply Eq (21) to obtain the wave drag coefficient of the body of revolution at that Mach number. (This is the body of revolution for which area distribution is given by $S(x_i) = S_i$ not A_i).

-- Repeat the procedure for each desired Mach number.

It is obvious from the above description that this procedure is exactly the full supersonic area rule when applied to a body of revolution. In order to validate the simplification proposed, Jumper applied the modified procedure to a number of controls. He showed that the simplified supersonic area rule exactly predicted the most favorable longitudinal

location to place a concentric protuberance on a given configuration (body of revolution). As he has pointed out, that result could not be attributed to his simplification but to the full supersonic area rule since the simplification, when applied on a body of revolution, is no longer simplification. Then he applied the procedure to aircraft configurations. He chose Models 1, 4, and 5 from Reference 18 for the following reasons:

a. Model 1 was a simple body of revolution for which his method should give the same results as the standard supersonic area rule;

b. Model 4 represented an example of moderately large areas located far off axis for which the supersonic area rule did a good job; and

c. Model 5 represented an extreme case of large areas located far off axis for which even the supersonic area rule began to fail (Ref 3:13).

His results for these three models are shown in Figure 9 (Ref 3). The results pertaining to the body of revolution were identical. The results for Model 4 were within a 20 percent accuracy at M = 1.1, and within 7 percent at M = 1.5, which may be considered a good result keeping in mind the simplification proposed. And, finally, the results for Model 5 were far off the experimental ones as were those from the standard supersonic area rule. In summary, for those configurations for which the standard supersonic area rule gives good agreement with experiment, it can be expected that his modified procedure would be able to predict the wave drag with reasonable accuracy.

It should be kept in mind that the comparison made was for the total zero-lift wave drag value -- not for increments of drag for which the modification was primarily proposed.

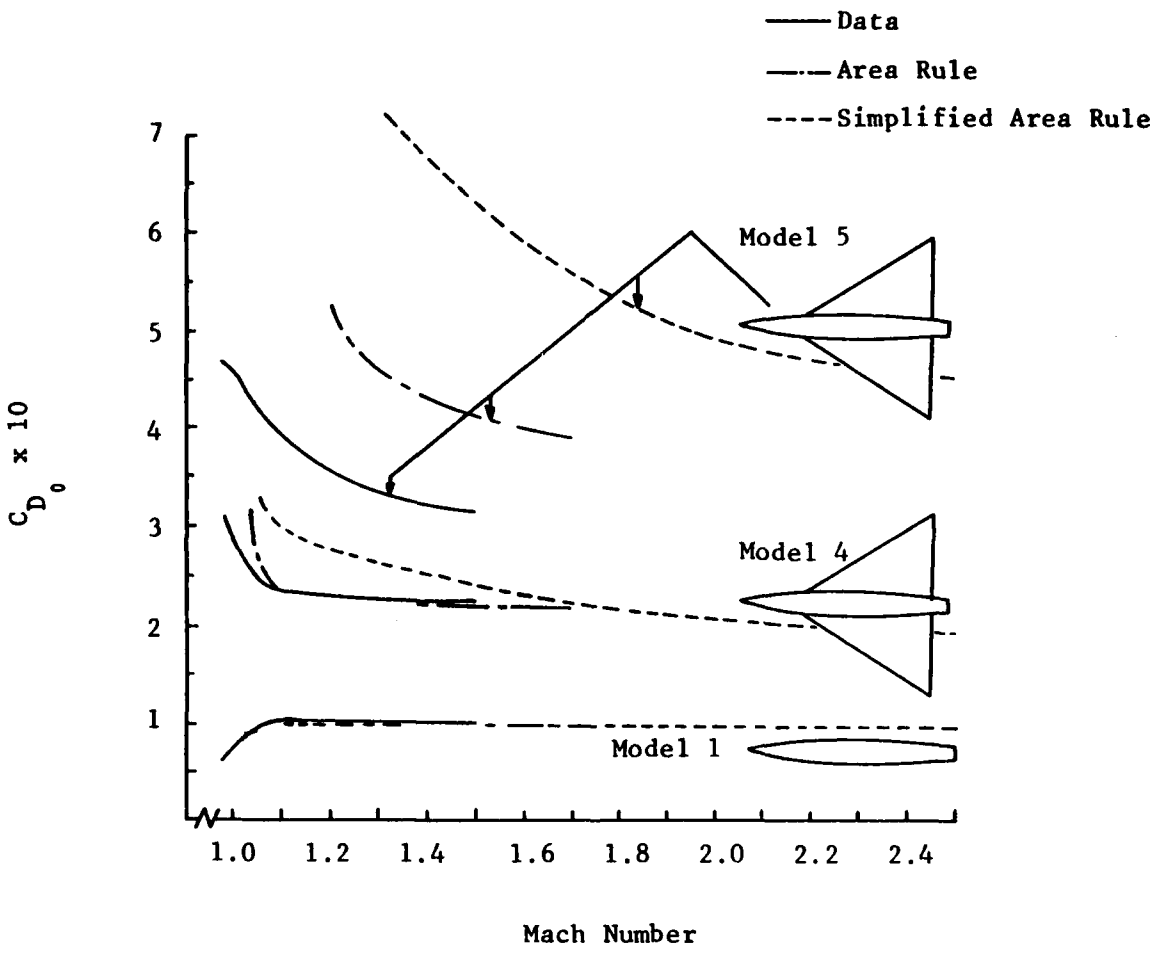

Figure 9. Comparison of Predicted Wave Drag at Zero Lift

Finally, Jumper applied the simplified method to predict wave drag increments by subtracting the results for an F-15 aircraft with and without two conformal McDonnell FAST PACK fuel pallets. The wave drag increment due to this configuration change was calculated and then compared to both wind tunnel data and supersonic area rule results. The results from the simplified algorithm were better than expected. This meant that this fast procedure should be further exploited.

Four New Proposed Simplifications of the Supersonic Area Rule

As stated in the Introduction, the purpose of the present work is two-fold, first to investigate new possible avenues of simplifying the supersonic area rule and second to further investigate the validity of the Jumper simplification. In fact, it might be said that the study is a comparison of four proposed schemes to that of Jumper.

The four new schemes are derived from the following consideration. The flow field around a three-dimensional body moving at supersonic speeds is conical in nature rather than planar. Owing to this fact, Quam (Ref 4) suggested that it might be interesting to try the following approach: Instead of using planes at different roll angles tangent to the characteristic Mach cone of the supersonic area rule, let us for the same purpose employ the cone itself. At a fixed Mach number, two Mach cones can originate at a point: One whose foremost point lies at that x location, the generators being directed down-stream -- this is the domain of influence for that point (x,0,0); and the other cone, directed up-stream -- the domain of dependence. By making use of the two Mach cones, several simplified approaches could be conceived.

Let us start as Jumper did with the whole structure of an actual aircraft collapsed to a single body of revolution as in Figure 10. Once the equivalent body of revolution (which has the same longitudinal cross-sectional area distribution normal to the airstream at zero incidence) has been constructed, then a Mach number of interest is chosen, say M_1. Referring to Figure 10, this Mach number defines a Mach cone with a half-angle, $\mu_1 = \text{Sin}^{-1}(1/M_1)$. The cone can be originated at any point on the body axis in either direction -- down-stream or up-stream. Let us consider the down-stream cone the vertex of which is at $x = x_m = m\Delta x$, where $m = 1,2,\ldots,n-1$ and $n = L/\Delta x$. The cone intersects the equivalent body of revolution making a cone with a height given by $t - x_m$. The lateral surface area of the cone (identified in Figure 10 as I) is designated S_m. Then the cone is moved further down-stream until its vertex reaches point $x = x_{m+1} = x_m + \Delta x = (m+1)\Delta x$, and a new area, S_{m+1}, is obtained in the same manner. Once the cone vertex has travelled through all the points starting from $x = x_1$ and finishing at $x_{n-1} = (n-1)\Delta x$, a set of areas $(S_1, S_2, \ldots, S_{n-1})$ is obtained. This set is then used to construct another equivalent body of revolution in such a way that the cross-sectional area formed by planes normal to the x - axis of this body at any x_m is exactly S_m. Then Eq (21) is applied to the former body and the wave drag coefficient is calculated using a scheme similar to that described earlier.

Another Mach number of interest, say M_2, defines a new Mach cone and the procedure is repeated yielding the wave drag coefficient that corresponds to M_2.

By looking at Figure 10 it can be recognized that the area designated by "I" was employed for the calculation described above. This scheme will

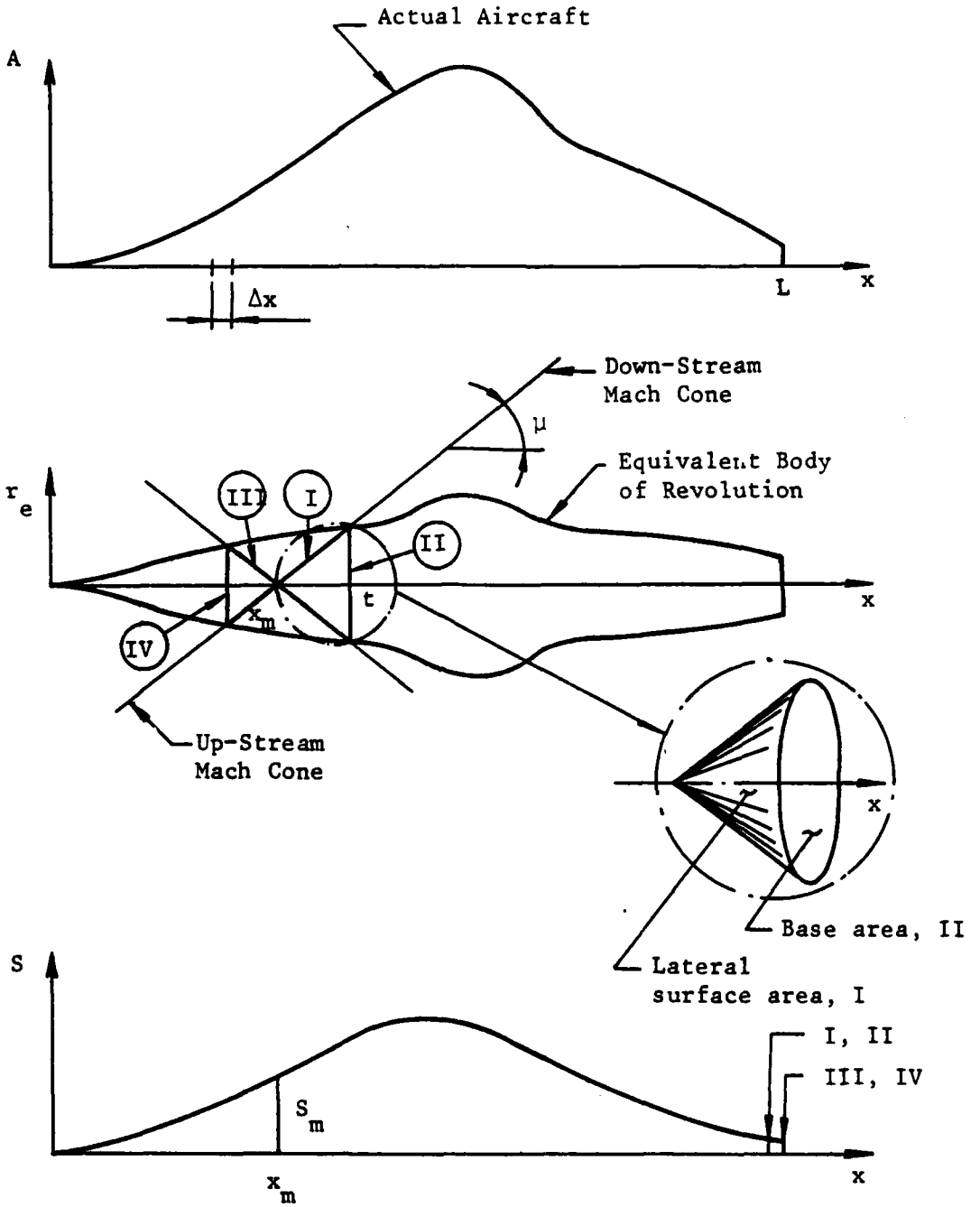

Figure 10. Four Versions of the New Proposed Simplification

be referred to as "Version I".

It should be pointed out that Version I does not employ any kind of projections of the cone surface area in obtaining the S_m's. Since the standard supersonic area rule employs the projections of S_m onto a plane normal to the body axis, a new set of projected areas may be defined and is marked by "II" on Figure 10. This new S_m is nothing but the base of the cone. When used in conjunction with Eq (21) these S_m yield a drag coefficient referred to as Version II.

It is easy to define two more versions, III and IV. Those were obtained basically the same way as Versions I and II -- the only difference being that the up-stream Mach cone was used. The total number of locations at which the cone vertex can lay for Versions III and IV was n instead of n-1 for the previous two versions, i.e., m = 1,2,. . .,n.

Since the four schemes described above shared the same starting point as Jumper's simplification (i.e., reducing a complex aircraft structure to a simple body of revolution), they preserved the two simplifying features of his modification -- a simple input data format and a need to perform only one integration for a particular Mach number of interest. Thus, there was no need to employ complex procedures such as a 3-D approximation and curve-fitting techniques as required in application of the full supersonic area rule algorithms (see for example Ref 13), where a 24-term Fourier series was used to calculate the slope of the area distribution.

A description of a computer program incorporating the methods detailed is included in Appendix I.

III. Results and Discussion

The programs described in Appendix I incorporating the four versions for wave drag prediction were employed to find the wave drag of a number of different aircraft configurations. Additionally, the wave drag predictions using the Jumper method were performed for comparison. About twenty different aircraft configurations were found in the literature which could serve as test cases more or less suitable for the purpose of the present study. (Unfortunately, not all of these aircraft data were available at the early stages of the present study. Because of time constraints, not all the configurations were analyzed.) After the first three aircraft were analyzed, it became clear (c.f. below) that Version II was the only one among the four new methods giving appropriately behaved C_{D_w} versus M curves. It was further noticed that the results obtained by employing Version II were about twice that which was expected. So, the results were arbitrarily multiplied by one half. The wave drag predictions employing the factor of one half will be referred to as the results from Version II' (see CDW2.F Program given in Appendix I). The results of all four versions initially, then Version II' only, and Jumper's method were compared to data obtained from free flight tests, wind tunnel tests, the standard supersonic area rule results whenever available for the configuration under consideration.

The following aircraft configurations were actually used as test cases:

-- McDonnell Douglas F-15 EAGLE with two conformal pallets the T-94 in place and without them

-- Fairchild F-105 REPUBLIC with the rear body bump and without it

-- Northrop F-5E (single seat) and F-5F (two seat) versions

-- Two V/STOL airplane configurations with wings of variable sweep

-- Two generic aircraft configurations as follows:

    -- Contoured body
    -- Full body

-- The effect of canopy location on the wave drag of a generic sweptback wing-body configuration, two configurations

-- Finally, a series of computations were run on a generic aircraft configuration to investigate the sensitivity of the results to the input data accuracy.

The results for each of the above cases will be described in detail within the following sections.

F-15 With and Without the Conformal Pallet T-94

The two configurations of the aircraft are described in Reference 3. Figure 11 shows the conformal pallet T-94 placed under the left wing of an F-15 aircraft, and Figure 12 shows the area distributions. The results of the investigation conducted by Jumper are given in Figure 13. The two configurations from reference 3 were run employing all four versions. The results obtained are presented in Figure 14 (no pallets -- clean F-15) and Figure 15 (with the pallets). The following can be said based upon these results:

-- The only method that gave the wave drag versus Mach number curve looking as it should was Version II.

-- The results obtained by employing what was termed as Version II looked reasonable, particularly at Mach numbers higher than M = 1.4.

Figure 16 shows the difference between the wave drag of the aircraft with the pallets in place minus the wave drag of the clean aircraft. It

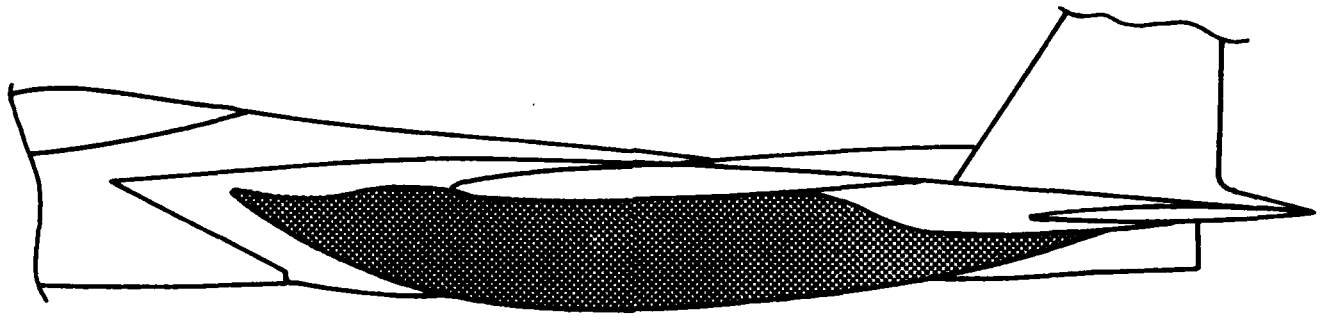

Figure 11. Location of the T-94 Pallet

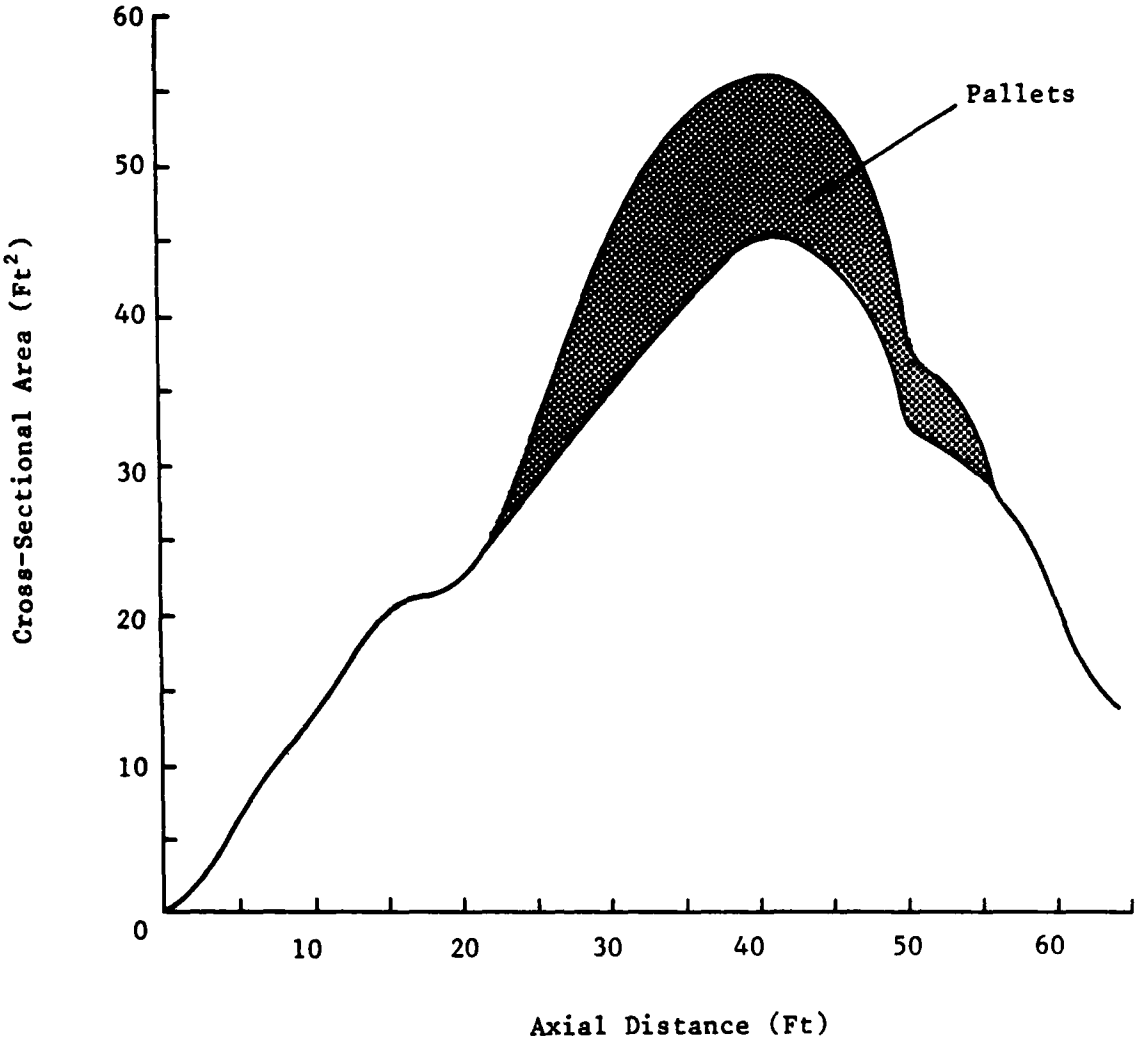

Figure 12. Area Distribution of the F-15 With and Without The Fast Pack Pallets Attached

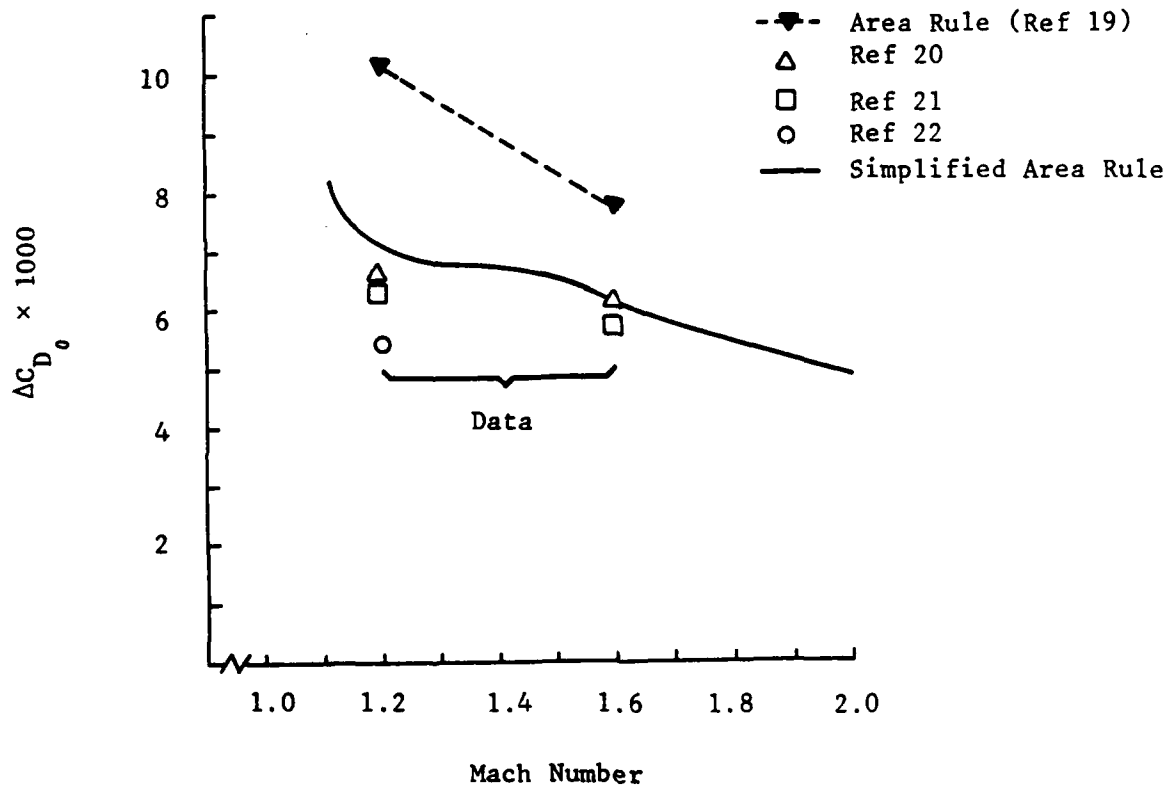

Figure 13. Incremental Drag Due to Adding The Fast Pack Fuel Pallets

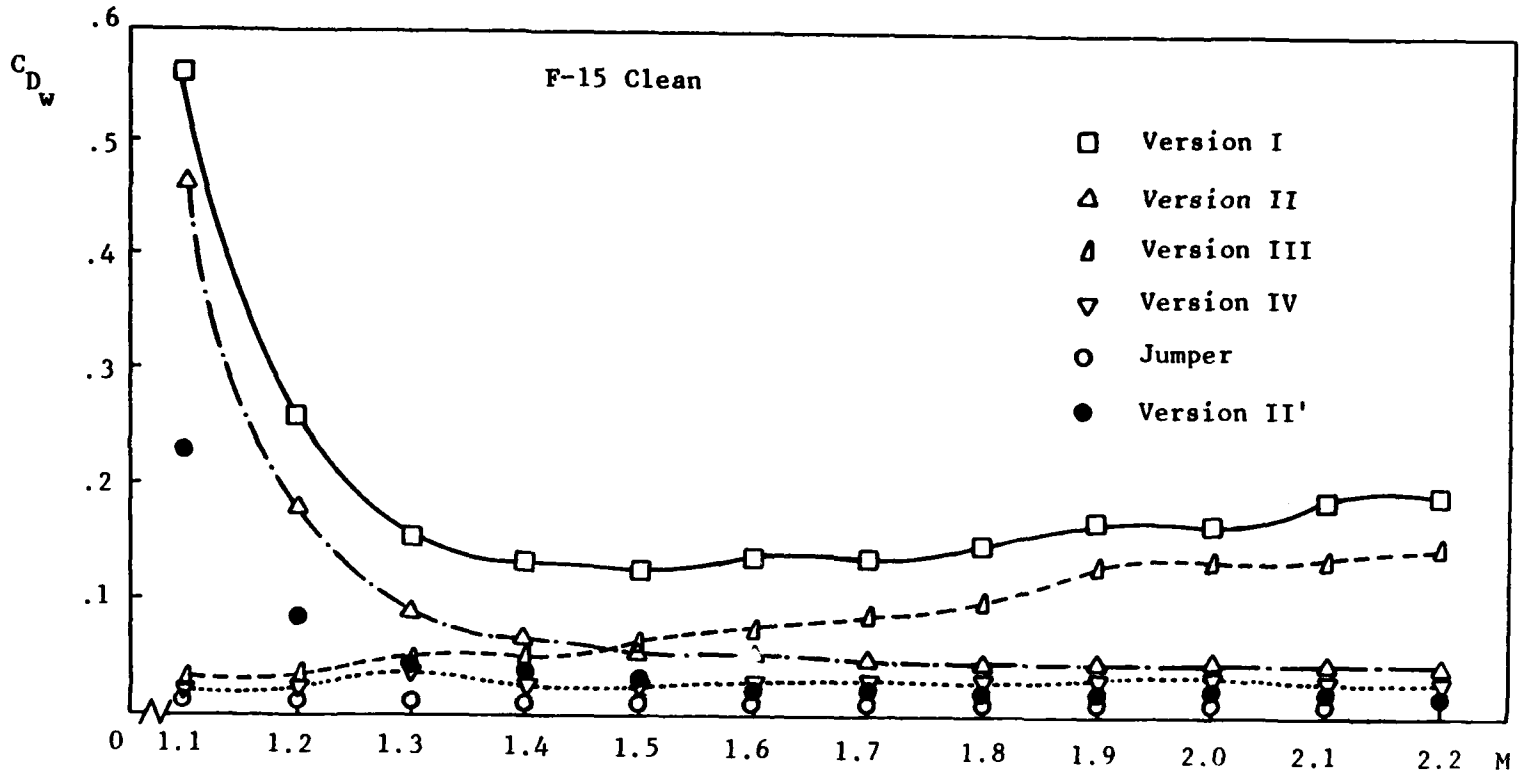

Figure 14. Predicted Zero-Lift Wave Drag of the F-15 Clean

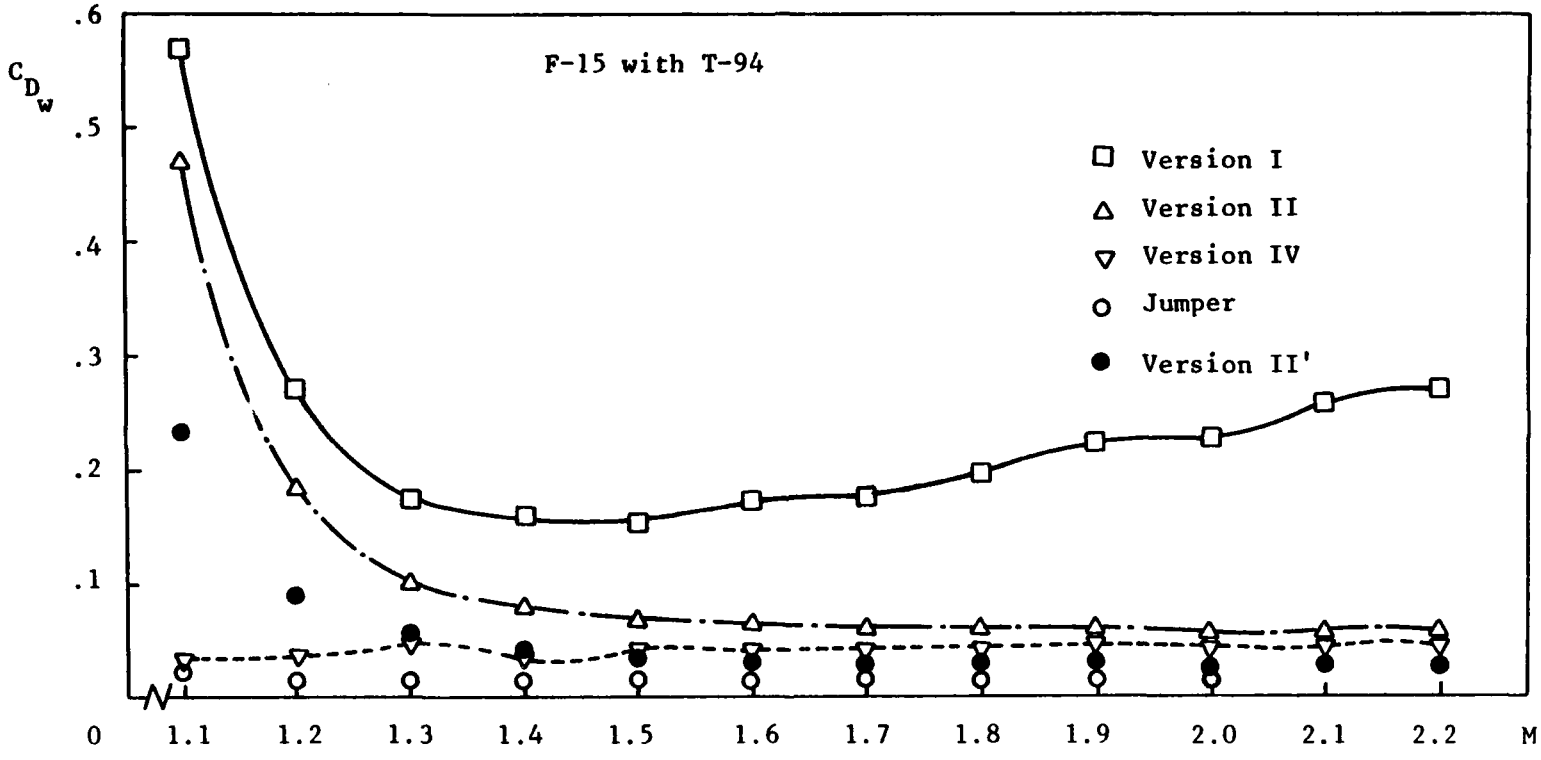

Figure 15. Predicted Zero-Lift Wave Drag of the F-15 With the T-94 Pallets

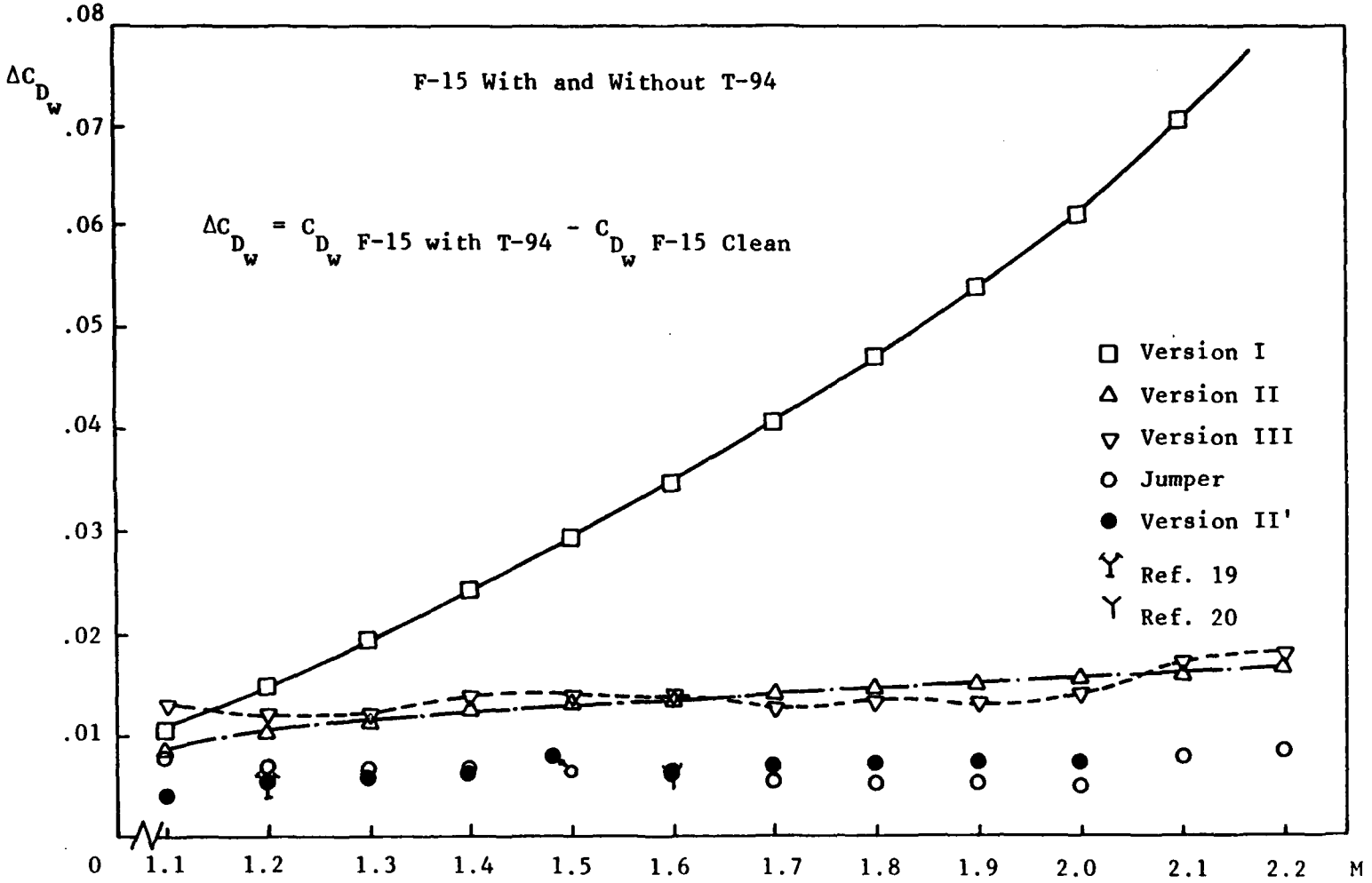

Figure 16. Incremental Drag Due to Adding the Pallets

can be seen that Version II' gave results very close to those from Jumper's study which were in excellent agreement with wind tunnel data available. Two values from references 19 and 20 almost coincided with the results of Version II' at the Mach numbers of 1.2 and 1.5. The results obtained by employing the other versions were too far off, particularly those from Version I (shown) and, even worse, from Version III (not shown since the values were so large -- of order of magnitude of 0.1 -- rather than to reduce the scale for the C_{D_w} to a meaningless one).

F-105 With and Without the Rear Body Bump

Description of the model of the aircraft can be found elsewhere (see for example references 23, 24, and 25).

Wind tunnel investigations have been conducted in the Langley 4- by 4-foot supersonic pressure tunnel at a Mach number of 2.01, and in the Langley 8-foot transonic tunnel at Mach numbers of 0.60 to 1.13. Several configurations (extended nose, wing root fairing, extended wing tips, added a rear body bump) have been tested; however, the only configurations for which the longitudinal cross-sectional area distribution data were available were the basic one and the one with the rear body bump added to improve the airplane drag characteristics at transonic speeds, the so-called "Mach-one bump". Figure 17 (Ref 23) shows the two configurations tested.

Figure 18 shows the wave drag coefficient results as obtained from the four versions and Jumper's simplification for the "bump off" configuration. Figure 19 shows the same kind of results from the same sources but now for the "bump on" configuration. Since the former two figures include both the wave drag data and minimum drag data from

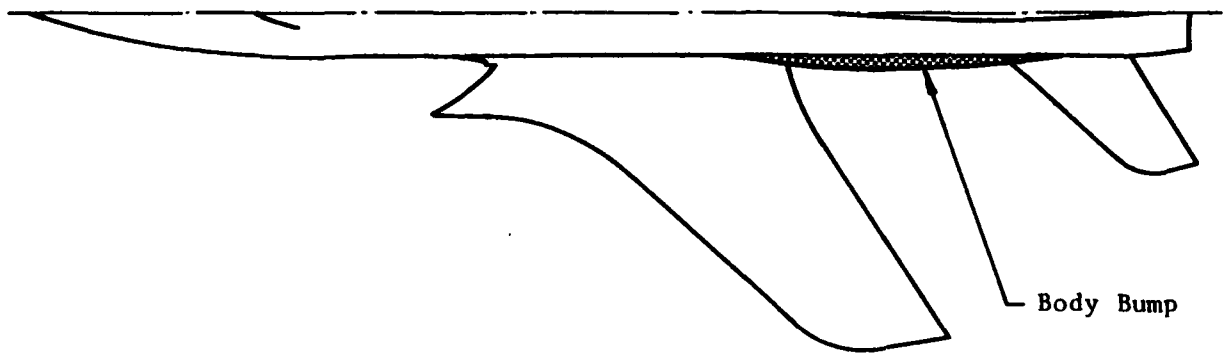

Figure 17. The F-105 REPUBLIC With and Without the Rear-Body Bump

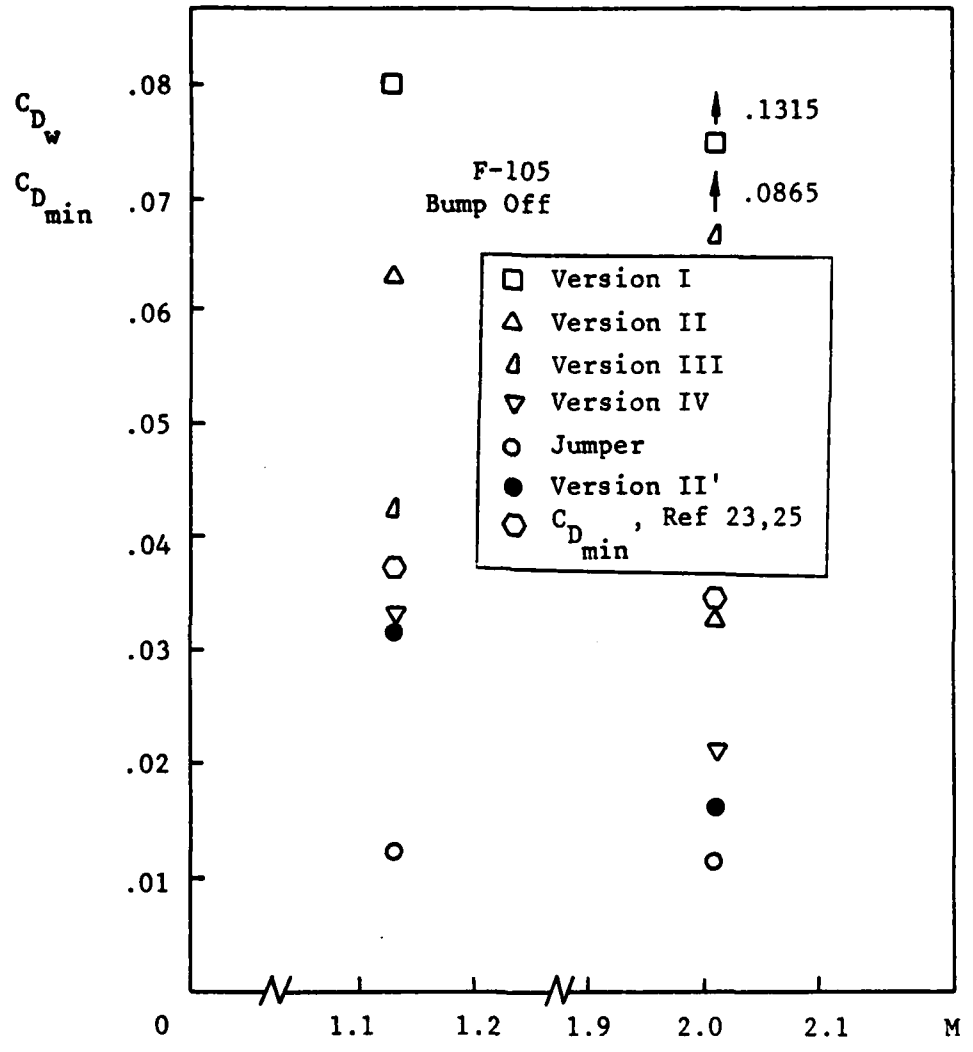

Figure 18. Some Predicted and Measured Drag Data of the F-105 Without the Rear Body Bump

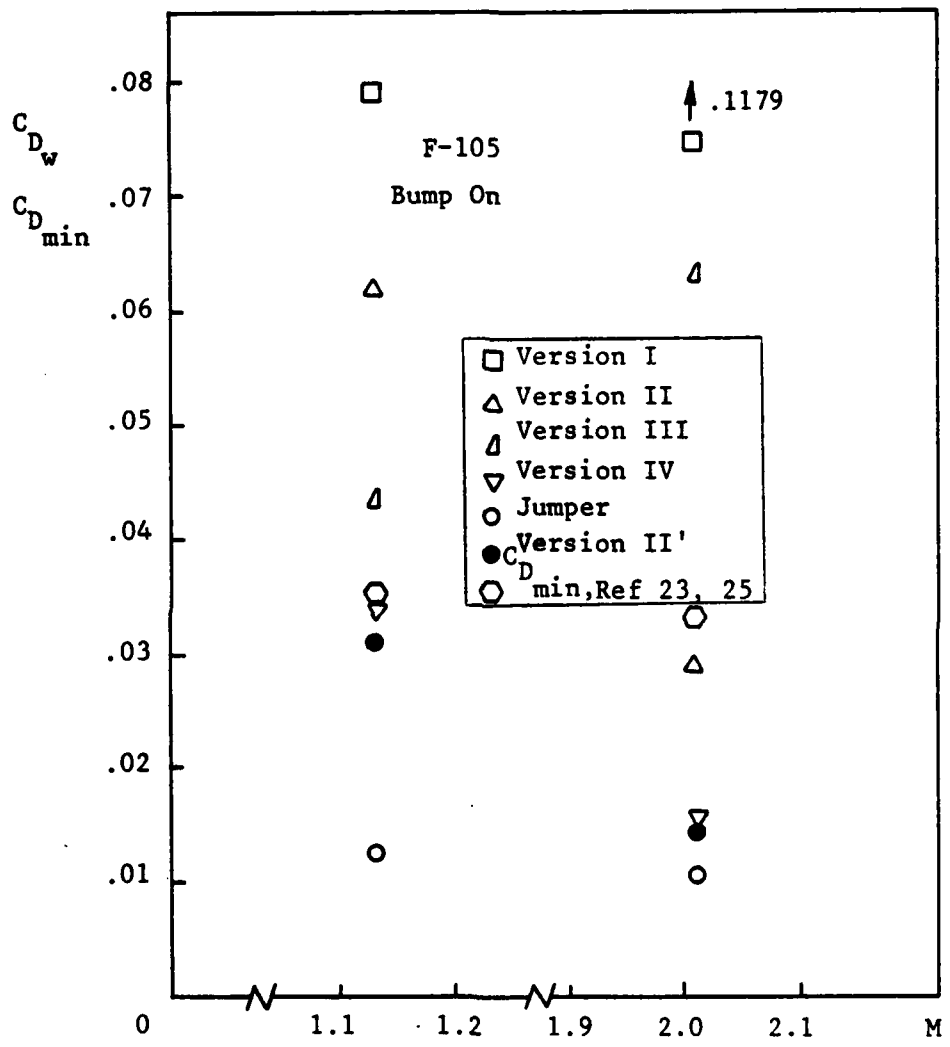

Figure 19. Some Predicted and Measured Drag Data of the F-105 Aircraft With the Rear Body Bump

references 23 and 25 at M = 1.13 and M = 2.01 respectively, the results are given in Table I containing the drag differences. The justification for such approach was that at zero angle of attack no flow separation would occur and therefore, the drag difference was basically due to the wave drag difference.

It can be seen from Table I that Jumper's simplification was the only modified approach able to give reasonable results, achieving a fourteen percent accuracy at M = 1.13 and even 9.97 percent relative error at M = 2.01. So, both the results from Jumper's method stayed below a fifteen percent accuracy limit. This agreement may be due to the way in which volume of the bump was added to the basic configuration -- namely as a concentrically placed volume increment which represents the most favorable case for Jumper's simplification. Remember that the simplification was primarily developed for investigation of near-to-axis-protuberances.

Northrop F-5E (Single Seat) and the F-5F (Two Seat) Versions

The first of these configurations used was the F-5E aircraft. The data for this aircraft, as found in reference 2, were the most complete for the purpose of this study since wave drag coefficient predictions over a range of Mach numbers of interest from M = 1.0 to M = 1.8 were available from two sources -- the 124J Wave Drag Program developed by the manufacturer, and the Langley Wave Drag Program. It should be pointed out that the Langley Program is generally used and accepted throughout the aircraft industry in the United States. Thus, relative errors were defined as being relative to the results from the Langley program.

Table I. F-105 With and Without the Rear Body Bump
(Zero-Lift Wave Drag Comparison)

ΔC_{D_w} From:							
M	I	II	III	IV	Jumper	II'	NACA*
1.13	.001	.0008	-.0017	-.0013	.00198	.0004	.0023
2.01	.0136	.0034	.0236	.0058	.00109	.0017	.0010

$\Delta C_{D_w} = C_{D_w \text{ Bump Off}} - C_{D_w \text{ Bump on}}$

and Compared to $\Delta C_{D_{min}}$ (NACA*, Ref 23 and 25)

Figure 20 shows the wave drag results for the aircraft obtained using the four versions and Jumper's modification. (It should be noted that the scale on the C_{D_w} axis is extremely small due to the large values for C_{D_w} obtained from Version III.)

Based on the results for the F-5 configuration the following two decisions were made:

1. To adopt the multiplier of one half as a permanent modification to Version II. This modification is justified solely by the success of its prediction capability and will be addressed again in a later section.

2. Not to employ any longer Versions I, III, and IV, since these appear to consistently predict incorrect C_{D_w} vs M curve shapes.

Figure 21 shows the wave drag coefficient values from the following methods: the Langley Program, the 124J Program, Jumper's simplification, and Version II. The relative errors of the three methods based on the values from the Langley program are shown in Figure 22. It can be seen from Figure 22 that the relative errors for both simplified methods stayed within limits of ten percent over a wide range of Mach numbers -- Jumper's method being superior at lower Mach numbers, up to M = 1.25, and Version II'over the rest of the range considered.

The data for the F-5F were not as complete as those for the single seat version (F-5E) and wave drag had to be estimated from the minimum drag coefficient. This was done in three different ways, the results of which are shown in Table II and Figure 23. The methods were as follows:

1. Using $C_{D_{min}}$ estimated by the Company and the wave drag for both planes as the same fraction (percentage) of the $C_{D_{min}}$.

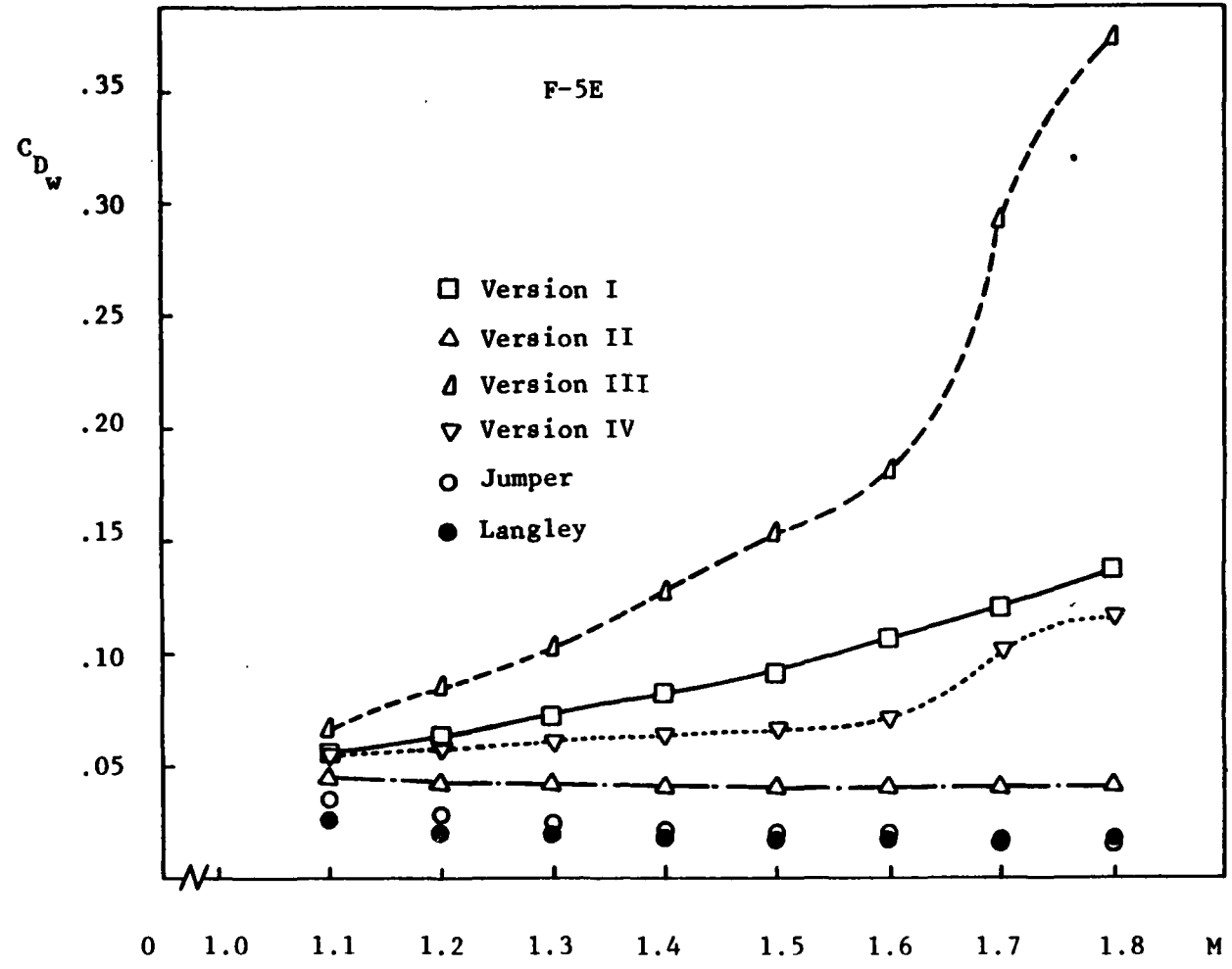

Figure 20. Predicted Zero-Lift Wave Drag of the F-5E Aircraft

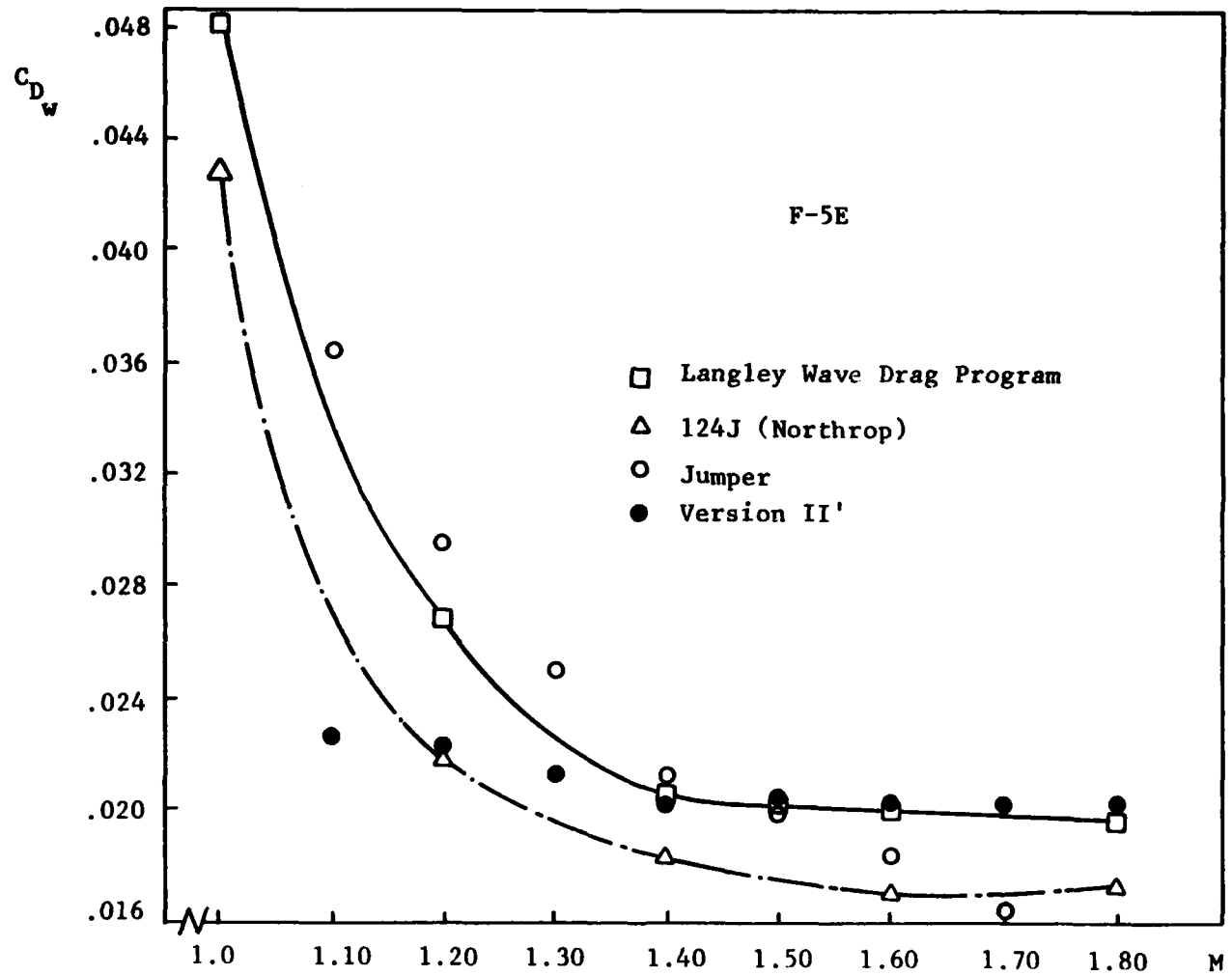

Figure 21. Comparison of Zero-Lift Wave Drag

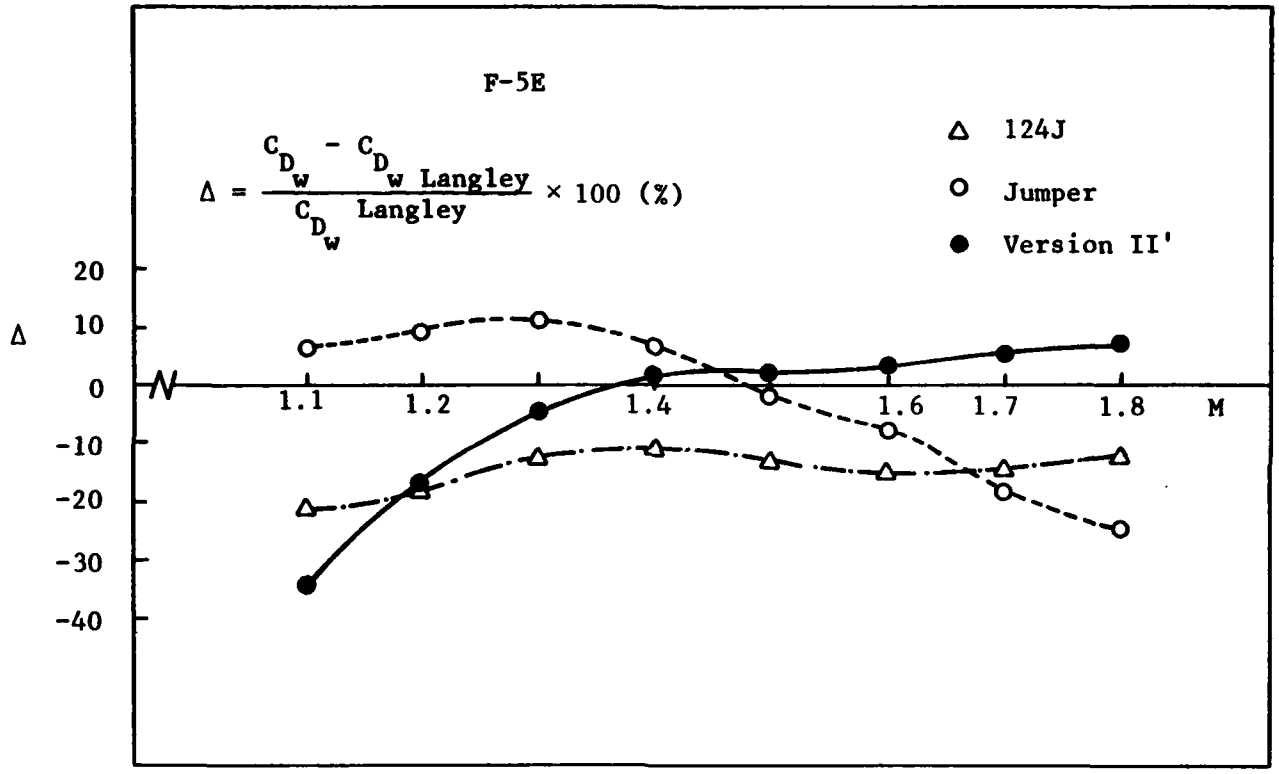

Figure 22. Relative Errors in Zero-Lift Wave Drag Data for the F-5E Aircraft

Table II. Zero-Lift Wave Drag Coefficient of the F-5F Aircraft

M	$C^F_{D_{wI}}$	$C^F_{D_{wII}}$	$C^F_{D_{wJ}}$	ΔJI	ΔJII	$C^F_{D_{wII'}}$	ΔII'I	ΔII'II
1.1	.039	.038	.0377	3.3%	- .79	.0236	39.5	37.9
1.2	.0319	.0304	.0306	4.2	- .49	.0230	28	24.5
1.3	.0274	.0258	.0259	5.7	- .2	.0221	19.5	14.5
1.4	.0254	.0241	.0225	11.4	6.6	.0215	15.4	10.8
1.5	.0251	.0244	.0203	18.9	16.8	.0216	13.8	11.5
1.6	.0248	.0247	.0187	24.6	24.4	.0217	12.5	12.3
1.7	.0245	.0245	.0163	33.5	33.4	.0220	10.2	10.1
1.8	.0243	.0248	.0149	38.6	39.9	.0224	7.6	9.7

Nomenclature:

$C^F_{D_{wI}}$ -- The wave drag coefficient for the F-5F aircraft as estimated by using flight test data for $C^F_{D_{min}}$

$C^F_{D_{wII}}$ -- The wave drag coefficient for the F-5F aircraft as estimated by using $C^F_{D_{min}}$ estimated (Northrop)

$C^F_{D_{wJ}}$ -- The wave drag coefficient for the F-5F aircraft as predicted using Jumper's simplified method.

$C^F_{D_{wII'}}$ -- The wave drag coefficient for the F-5F aircraft as found by using Version II'

Δxy -- The relative error, data from an x source relative to y source:

$$\Delta xy(\%) = \frac{C^F_{D_{wx}} - C^F_{D_{wy}}}{C^F_{D_{wy}}} \times 100$$

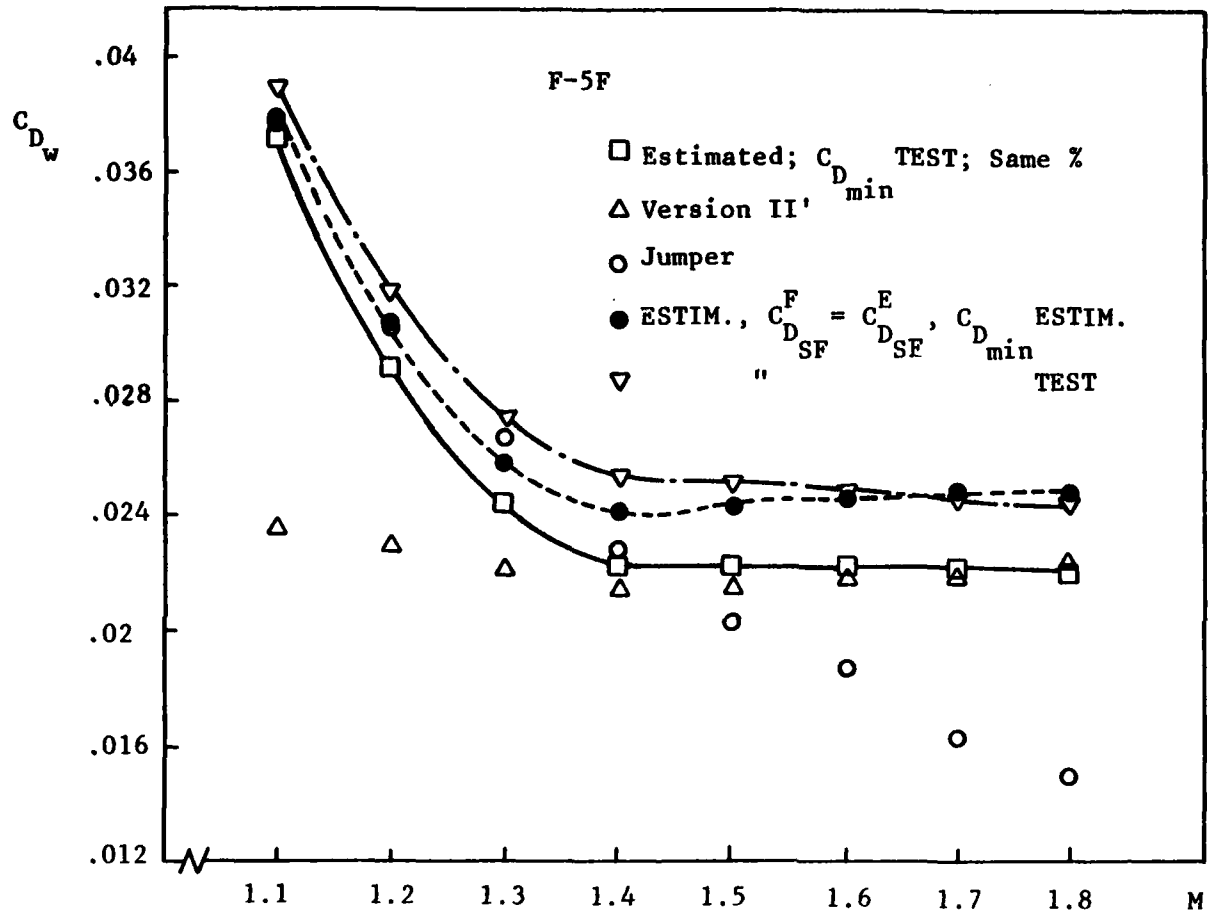

Figure 23. Comparison of Zero-Lift Wave Drag Data For the F-5F Aircraft

2. Equating the skin friction drag coefficients for both aircraft and using $C_{D_{min}}$ as estimated by the Company ($C^F_{D_w}$ II).

3. Equating the skin friction again but now using $C_{D_{min}}$ as obtained from flight tests ($C^F_{D_w}$ I).

It can be seen from Figure 23 that Jumper's simplification gives good results at Mach numbers up to M = 1.35 -- within ten percent accuracy. The results obtained from Version II' correlated to both flight test data and those estimated by Northrop better at higher Mach numbers, M = 1.40 to 1.80.

Two V/STOL Airplane Configurations With Wings of Variable Sweep

Two unconventional aircraft configurations were studied to see what kind of results could be expected. These two were V/STOL airplane configurations with wings of variable sweep. The models of the aircraft are described in reference 26 as Models I and II. These two configurations were chosen because their unconventional shapes differed significantly from the usual limitations imposed on the use of the supersonic area rule. The models were in a 1/10 scale and Mach number range was from M = 1.10 to M = 1.30. The C_{D_0} data were available from the wind tunnel tests described in reference 26.

Table III shows the results obtained by employing both Jumper's modification and Version II' up to M = 1.3. It was assumed that no separation occurs and the differences in the C_{D_0} data were basically due to difference in the wave drag data pertaining to the two configurations. That is why C_{D_w} from the simplifications was compared directly against C_{D_0} from the wind tunnel drag pclars.

Table III. Wave Drag Characteristics of Two V/STOL Aircraft

M	Model 1			Model 2			ΔC_D		
	C_{D_0}	C_{D_w}		C_{D_0}	C_{D_w}		ΔC_{D_0}	ΔC_{D_w}	
	Tunnel	Jumper	II'	Tunnel	Jumper	II'	Tunnel	Jumper	II'
1.1	.0427	.0341	.0262	.0445	.0371	.0269	.0018	.003	.0007
1.2	.0413	.0269	.0265	.0443	.0304	.0271	.0030	.0035	.0006
1.3	.0437	.0237	.0267	.045	.0276	.0273	.0013	.0039	.0006

It can be seen from Table III that neither of the methods correlated well to the wind tunnel measurements. The closest result found was that for M = 1.20 obtained by using Jumper's simplified method, with a relative error of 16.7 percent. Further, Version II gave even a wrong looking C_{D_w} vs M curve as the wave drag coefficient was increasing with increasing Mach number over the range investigated.

The reasons for the results just described might be as follows:

1. Low wind tunnel data accuracy (± 0.001) which affects directly the C_{D_0} compared to. The disagreement between the results from Jumper's simplification and the wind tunnel data is probably -- but only partially -- due to this fact.

2. The second, more important reason, is as follows:

> Let us suppose we have a simplified method ("first generation simplification") applicable to a restricted class of problems, and when applied to a problem that does not belong to the restricted class, the simplification gives highly erroneous results. Let us go a step further and simplify the simplification -- we will get a kind of "second generation simplification". Obviously, it will be restricted to an even smaller group of problems. But what will happen if for any reason we try to employ our second generation simplification to solve a problem which was "out of reach" even for the first generation simplification? What quality can we expect from our results? The answer is: None. That is exactly the case in investigating these aircraft by applying the simplifications of the full supersonic area rule to the configurations which were very different from those to which Jones restricted his result -- the supersonic area rule. Essentially, Jones restricted

his formula to thin wings centrally mounted on a slender body type fuselage (see Ref 11:2). The two aircraft, having a six percent thick, shoulder mounted wing, clearly fall outside these restrictions.

Two Aircraft Configurations Designed For Different Mach Numbers

Two aircraft configurations employing sweptback (60 degrees) wings which were cambered and twisted and mounted in a mid-position were investigated. The two configurations are described in reference 8. These were chosen for investigation because, being designed for specific Mach numbers, they had the zero-lift drag versus Mach number curves which offered the lowest drag at the design Mach numbers of 1.0 and 1.4.

No reasonable results were obtained in this case. In my opinion, this failure of both simplifications to correlate well to the wind tunnel results could have been due to a low accuracy of input data available; two extremely small figures (less than three by two inches) showing the aircraft longitudinal cross-sectional area distributions were available. It is interesting to note, however, that the two simplified methods failed differently:

-- Jumper's simplification preserved the C_{D_w} vs M curve shape while giving about two times lower C_{D_w} values than the data (e.g., C_{D_w} = .0033 at M = 1.10).

-- Version II shows oscillations in the C_{D_w} values at M = 1.10 to 1.40.

The wing thickness which varied from 12 percent at the wing root to six percent at the 50 percent semispan section and then remained

constant to the tip might also be a factor of secondary importance in this case; yet, no doubt the existence of such a thick wing would have affected the results even if more accurate input data were available (Ref 8).

The mentioning of this case was intended to illustrate how crucial accuracy of an input data set is to the quality of the results. This indication motivated the limited investigation of the results sensitivity to the input data accuracy which will be described in a later section.

Two Delta Wing-Body Combinations Contoured as Specified by the Transonic Area Rule

Two delta wing-body combinations contoured according to the transonic area rule to reduce the zero-lift drag at Mach numbers of 1.41 and 2.01 were investigated. The two configurations are described in reference 27.

1. Full body which was a body of revolution of optimum shape or the given length, maximum diameter, and base diameter.

2. Contoured body which was constructed according to the transonic area rule so that the total cross-sectional area of the wing-body combination at any station was the same as that of the optimum full body alone.

Both of these bodies had the same wing.

Additional configurations were described in reference 27; however, these configurations had inconsistencies in the body shape variables and the presence of the faired inlets, and so were not used.

The two configurations investigated are shown in Figure 24 and the results obtained are given in Table IV.

It can be seen from Table IV that an excellent agreement in the ΔC_D data at M = 1.41 was obtained by using Version II. At the higher

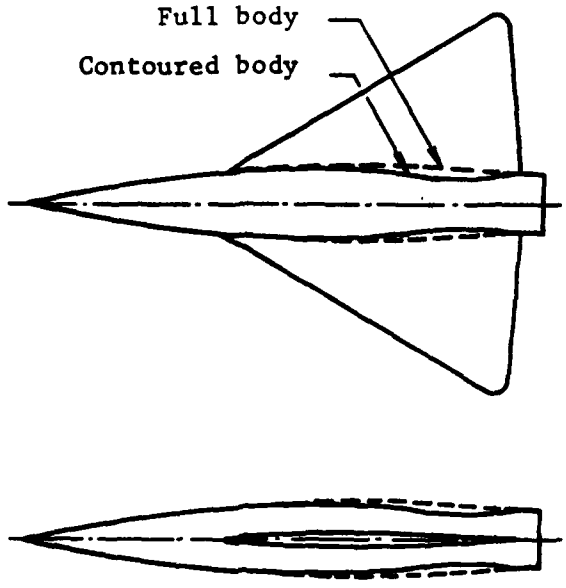

Figure 24. Two Generic Aircraft Configurations

Table IV. Zero-Lift Drag Differences For Two Generic Aircraft

M source	Wind Tunnel	Jumper	Version II'
1.41	.003	.0071	.0029
2.01	.0008	.0046	.0038

$$\Delta C_{D_0} = C_{D_0 \text{ Full Body}} - C_{D_0 \text{ Contoured Body}}$$

Mach number differences in C_{D_0} were small -- of the order of magnitude of the tunnel measurements error (± .0005) and no agreement was achieved by using either of the modifications. On the other hand, these configurations were of the type to which Jumper's simplification has already been applied without success (large areas located far off the axis -- see Section II, Simplifications to the Supersonic Area Rule.

The Effect of the Canopy Location on the Wave Drag of a Sweptback Wing-Body Configuration

The effect of canopy location for a sweptback wing-body combination designed to fly at transonic speeds was investigated by considering the following two cases (Ref 28):

1. The canopy placed on the body so that the cross-sectional area of the canopy approximately filled the concave portion of the basic wing-body cross-sectional area distribution (design location), and

2. The canopy placed 0.0614 of the body length forward of the design location.

Along with the two configurations, the basic wing-body (no canopy) configuration was investigated.

The wind tunnel data showed a significant drag reduction for configuration #1. Table V shows the results obtained by employing the two simplified methods. It can be seen from the table that Jumper's simplified method gave very good results for a number of cases, particularly in predicting the wave drag increment due to moving the canopy from the forward to the rear (design) position. Keeping in mind that the wind tunnel data accuracy was ± .0005, Jumper's modification showed not only the right trend in the wave drag changes, but actually

Table V. The Effect of the Canopy Location on Zero-Lift Drag Of a Sweptback Wing-Body Combination

M →	1.05			1.10			1.15		
Source →	Wind Tunnel	Jumper's Method	Version II'	Wind Tunnel	Jumper's Method	Version II'	Wind Tunnel	Jumper's Method	Version II'
$C_{D_{w\ F.C.}}^{*} - C_{D_{w\ W-B}}$	.001	.001	.0007	.001	.007	.0008	.0011	.0005	.0007
$C_{D_{w\ F.C.}} - C_{D_{w\ R.C.}}$	.0016	.0013	.0004	.0015	.0014	.0006	.0013	.0014	.0004
$C_{D_{w\ R.C.}} - C_{D_{w\ W-B}}$	-.0006	-.0003	.0003	-.0005	-.0007	.0002	-.0002	-.0009	.0003

F.C = Forward Canopy
R.C.= Rear Canopy
W-B = Wing-Body

* → or: C_{D_0} for the Wind Tunnel Data

$\Delta C_D = \pm .0005$

predicted the reduction in the wave drag by the addition of the canopy at the design position when compared to the wing-body alone.

Version II' failed to give any reasonable results in this case. The reasons for this failure will be discussed in Chapter IV.

Sensitivity of the Results to the Input Data Accuracy

As mentioned previously, the results of Section - Two Aircraft Configurations Designed for Different Mach Numbers, suggested the need for at least a limited investigation of the sensitivity of results to the input data accuracy. Thus, the input data set for the F-5E was used for this purpose since the data pertaining to that aircraft were the most complete data available.

The sensitivity was investigated by calculating the wave drag coefficient using input data $A(x_i)$ which were modified in a random way within ± 5 percent limits.

The results of this investigation are presented in Table VI. It would not be justified to draw general conclusions based upon this single case but it should be pointed out that the sensitivity of Version II' was considerably higher (i.e., the CDW2 Program was less tolerant) than the Jumper method. The reason this might lie in the less regular behavior of the area distribution when the Mach cone lateral surface is employed rather than that obtained by making use of Mach planes. This can be explained with the aid of Figure 25. If we approximate the first derivative of the area distribution as

$$S'(x_m) \simeq (S_{m+1} - S_m)/(x_{m+1} - x_m)$$

Table VI. Sensitivity of the Results to The Input Data Accuracy

M	Jumper			Version II'		
	C_{D_w} 'Exact' Data	C_{D_w} ±5% Er.	Δ (%)	C_{D_w} 'Exact' Data	C_{D_w} ±5% Er.	Δ (%)
1.1	.0366	.0395	+ 7.9	.0227	.0314	38.3
1.2	.0296	.0325	9.8	.0222	.0305	37.4
1.3	.0250	.0282	12.8	.0213	.0302	41.8
1.4	.0218	.0245	12.4	.0207	.0297	43.5
1.5	.0198	.0220	11.1	.0206	.0302	46.6
1.6	.0184	.0205	11.4	.0207	.0299	44.4
1.7	.0161	.0181	12.4	.0209	.0287	37.3
1.8	.0149	.0163	9.4	.0212	.0330	55.7
1.9	.0140	.0148	5.7	.0212	.0289	36.3
2.0	.0134	.0136	1.5	.0204	.0294	44.1

$$\Delta(\%) = \frac{C_{D_{w\ \pm 5\%}} - C_{D_{w\ \text{'Exact' Data}}}}{C_{D_{w\ \text{'Exact' Data}}}} \times 100$$

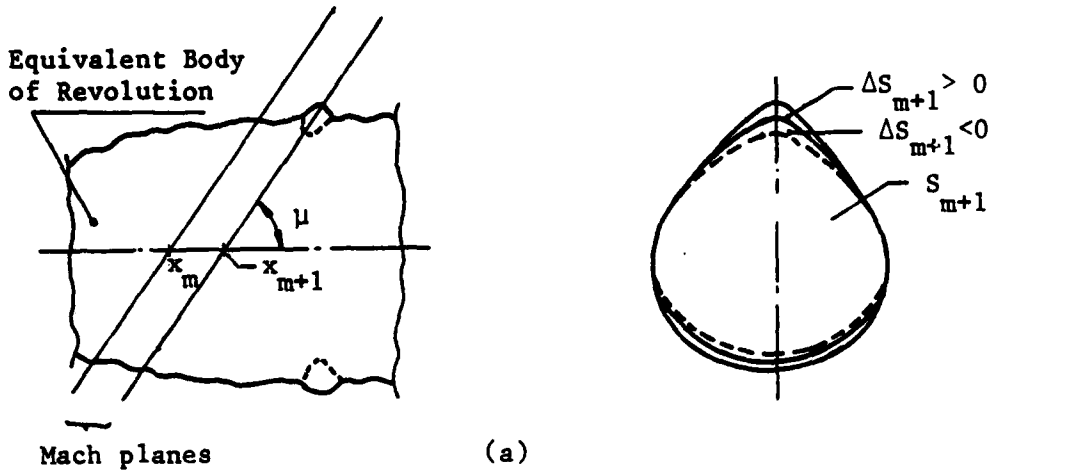

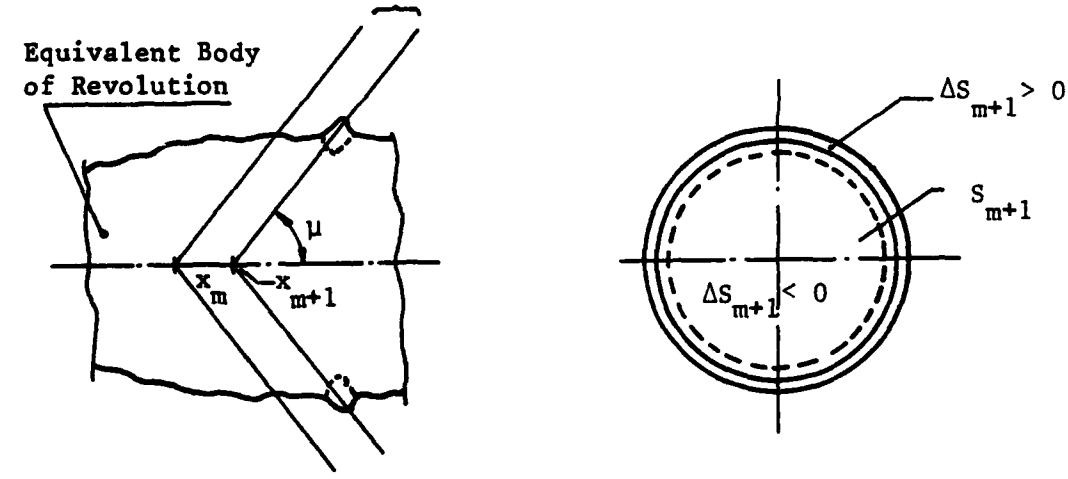

Figure 25. The Input Data Error Effects

(a) Jumper's Method

(b) Version II'

where $S_{m+1} = S_{m+1}$ exact + ΔS_{m+1} , it is obvious that a larger ΔS_{m+1} in the case of the CDW2 Program will create larger deviations in the S'(x) values and therefore, in the final result, the C_{D_w} value. An analogous situation occurs when ΔS_{m+1} is negative. In the case of Jumper's procedure, random errors will tend to be cancelled out and it might, therefore, be more forgiving.

A more systematic investigation should be conducted along this line.

IV. Theoretical Reasoning for the Results Obtained

At the beginning of the present study, some indications, mostly of an intuitive nature, existed suggesting that employing of the Mach cone surfaces in a supersonic-area-rule-type procedure might lead to some interesting results. The rationale for this situation was contained in the fact that supersonic flow fields are, by their nature, more conical than plane, and the higher Mach number we consider, the more conical the flow field becomes.

The cases investigated have shown usefulness of the method and a number of cases gave very good results, especially when one keeps in mind the degree of the simplification proposed. On the other hand, the simplified method proposed by Jumper appears to be generally superior to Version II' when considered over the entire range of Mach numbers investigated and showed particularly good correlation to full supersonic area rule predictions at lower Mach numbers. However, it can be stated firmly, based upon this limited investigation, that Jumper's method correlated better at lower Mach numbers while Version II did a better job at moderate Mach numbers, from $M = 1.4$ to, approximately, $M = 2.0$. My explanation for this is as follows. Basically what Jumper did is combined an extended transonic area rule with the full supersonic area rule. Thus, one would expect that the closer the Mach number is to unity (from above) the better the results. Thus, it is not surprising that Jumper's method proved to be superior over Version II' at lower, basically transonic Mach numbers. On the other hand, the supersonic flow field becomes more conical as Mach number is increased. This might be the rationale why

employing the Mach cones, instead of planes, gives better results at higher Mach numbers.

It should be pointed out that in applying either Jumper's method or Version II', a user cannot neglect the restrictions which must hold for the full supersonic area rule in order to expect any meaningful results. Within these restrictions (as was the case for the F-5E aircraft with its thin wing of small area, both simplified methods gave good results for the aircraft, each method within its "favorable" Mach number range) one might expect reasonable results.

Finally, no reason other than success in predicting wave drag could be found for multiplying by one half times the results from Version II'. Attempts to explain an apparently arbitrary factor were not successful. So, this factor remains unexplained. It should be remembered, however, that the supersonic area rule has a history of unexplained procedures which are justified only by success. For example, the standard supersonic area rule uses the frontal projections of oblique area rather than the oblique areas themselves (Ref 3) which are the areas that should be used from the theory (Ref 11).

V. Conclusions

A modified method of the supersonic-area-rule-type was developed. Instead of using the axis normal projection of the area cut by the oblique Mach planes through the full aircraft configuration suggested by Jones, Lomax, and Whitcomb, the down-stream Mach cone lateral surface was used on the equivalent body of revolution of the configuration. A computer program to perform the required calculations according to this modified procedure was written. Several cases of actual aircraft configurations and wind tunnel models were used for numerical investigation of the method. Some promising results were found along with tremendous decreases in both core storage and computing time required by the full supersonic area rule.

The following conclusions were indicated:

1. The modified method correlated well, particularly at moderate supersonic Mach numbers (from M = 1.4 to M = 2.0).

2. Like the supersonic area rule the best correlation was achieved when dealing with thin wings centrally mounted on a slender fuselage.

3. The method proposed by Jumper proved superior to the new simplification at transonic and lower supersonic speeds; however, the new method appears to be superior at the higher Mach numbers.

4. The new simplification showed a high level of sensitivity to the input data set quality -- input deviations of less than five percent brought about untolerable discrepancies in the wave drag values.

5. Further investigations of the method are necessary prior to its general acceptance for quick and reasonable accurate zero-lift wave drag calculations.

Bibliography

1. Harris, R. V. Jr., "An Analysis and Correlation of Aircraft Wave Drag", TM X-947, NASA, 1964.

2. Chao, D., Northrop Corporation, Aircraft Group, Private communications - letters: 15 June 1983 and 18 August 1983.

3. Jumper, E. J., "Wave Drag Prediction Using a Simplified Supersonic Area Rule", Journal of Aircraft, Vol. 20, No. 10, October 1983, pp. 893-895.

4. Quam, D. L., Private communication.

5. Ashley, H., and Landahl, M. T., Aerodynamics of Wings and Bodies, Addison-Wesley Publishing Company, Inc., Reading, Massachusetts, 1965, pp. 173-179.

6. Jones, R. T., "Theory of Wing-Body Drag at Supersonic Speeds", Report 1284, NACA.

7. Liepman, H. W., and Roshko, A., Elements of Gas Dynamics, John Wiley & Sons, New York, 1957, pp. 235-239.

8. Whitcomb, R. T., and Sevier, J. R. Jr., "A Supersonic Area Rule and An Application to the Design of a Wing-Body Combination with High Lift-Drag Ratio", Technical Report R-72, NASA, 1960.

9. Leyman, C. S., and Markham, T., "Prediction of Supersonic Aircraft Aerodynamic Characteristics", AGARD-LS-67, 1974.

10. Donlan, J. C., "An Assessment of the Airplane Drag Problem at Transonic and Supersonic Speeds", RM L54F16, NACA, July 1954.

11. Lomax, H., "The Wave Drag of Arbitrary Configurations in Linearized Flow as Determined by Areas and Forces in Oblique Planes", RM A55A18, NACA, 1955.

12. Hayes, W. D., "Linearized Supersonic Flow", Rep. No. AL-222, North American Aviation, Inc., June 18, 1947.

13. Whitcomb, R. T., "A Study of the Zero-Lift Drag-Rise Characteristics of Wing-Body Combinations Near the Speed of Sound", Report 1273, NACA.

14. Lomax, H., and Heaslet, M.A., "Recent Developments in the Theory of Wing-Body Wave Drag", Journal of the Aeronautical Sciences, Vol. 23, No. 12, December 1956.

15. Spreiter, J. R., "Aerodynamic Properties of Slender Wind-Body Combinations at Subsonic, Transonic and Supersonic Speeds", Technical Note 1662, NACA.

16. Baals, D. D., et al, "Aerodynamic Design Integration of Supersonic Aircraft", Journal of Aircraft, Vol. 7, No. 5, September-October 1970.

17. Smith, N. F., et al, "Drag of External Stores and Nacelles at Transonic and Supersonic Speeds", RM L53I23b, NACA, October 1953.

18. Nelson, R. L., and Welsh, C. J., "Some Examples of the Applications of the Transonic and Supersonic Area Rules to the Prediction of Wave Drag", Technical Note D-446, NACA.

19. Lemley, C.E., Triplett, W. E., Verhoff, A., "Aerodynamic Interference Due to Optical Turrets", Flight Dynamics Laboratory Report, AFWAL-TR-80-3058, Air Force Wright Aeronautical Laboratories, September 1978.

20. Meyer, W. L., "Summary of Results of Series XI Polysonic Wind Tunnel Tests on 4.7% Scale Model of the Model 199A-PSWT Test #366", Report MDC 4589, December 1976, McDonnell-Douglas Aircraft Co., St. Louis, Missouri.

21. Meyer, W. L., "Summary of Results of Series XI Polysonic Wind Tunnel Tests on 4.7% Scale Model of the Model 199A-PSWT Test #361", Report MDC A4405, September 1976, McDonnell-Douglas Aircraft Co., St. Louis, Missouri.

22. Riley, D. R., "Results of F-15 CFT Store Station Wind Tunnel Test with MK-82 Low-Drag General Purpose and MK-84 Laser-Guided Bombs", Report MDC A5907, April 1979, McDonnell-Douglas Aircraft Co., St. Louis, Missouri.

23. Luoma, A. A., "Investigation of a 1/22-Scale Model of the REPUBLIC F-105 Airplane in the Langley 8-Foot Transonic Tunnel; Lateral, Directional, and Longitudinal Static Stability and Control", RM SL57H06, MACA, August 1957.

24. Luoma, A. A., "Investigation of a 1/22-Scale Model of the REPUBLIC F-105 Airplane in the Langley 8-Foot Transonic Tunnel; Static Longitudinal Stability and Control and Performance Characteristics at Transonic Speeds", RM SL56D12, NACA, April 1956.

25. Spearman, M. L., et al, "Aerodynamic Characteristics of Various Configurations of a Model of a 45 Degree Swept-Wing Airplane at a Mach Number of 2.01", RM L54J08, NACA, 1955.

26. Luoma, A. A., et al, "Performance, Stability and Control Characteristics at Transonic Speeds of Three V/STOL Airplane Configurations with Wing of Variable Sweep", TM X-321, NASA, October 1960.

27. Carlson, H. W., "Preliminary Investigation of the Effects of Body Contouring as Specified by the Transonic Area Rule on the Aerodynamic Characteristics of a Delta Wing-Body Combination at Mach Numbers of 1.41 and 2.01", RM L53003, NACA, 1953.

28. Robinson, H. L., "The Effect of Canopy Location on the Aerodynamic Characteristics of a Swept-Back Wing-Body Configuration at Transonic Speeds", RM L54E11, NACA, June 1954.

Appendix I. Description of the Computer Programs Written To Incorporate New Simplifications

A general flow chart type description of the procedures described in Section 2 - Four New Proposed Simplifications of the Supersonic Area Rule, is shown in Figure 26.

This procedure was translated into a computer program for calculating a wave drag coefficient and a listing of one such program for Version II' is given in Appendix I (the CDW2 Program).

Prior to performing any actual calculation, a set of input data had to be read in. The set includes the following:

n -- The number of steps along the aircraft longitudinal axis. It was recommended in reference 3 to keep this number about 100 for both accuracy and processing time requirement reasons. In the calculations performed n was being given values between 64 and 128.

L -- The aircraft length.

sref -- Some reference area, usually the wing planform area.

machs -- The lowest Mach number at which the user wants to calculate the wave drag coefficient.

machf -- The highest value of Mach number at which the wave drag is to be calculated.

nm -- Number of Mach number steps in between machs and machf.

(Given machs, machf and nm the Mach number step size is calculated as: dmach = (machf - machs)/nm.)

The next thing to be entered was:

A(i) -- The cross-sectional areas obtained by cutting the configuration by planes normal to the aircraft longitudinal axis. The A(i)'s require a double precision format since the IMSL routines on the VAX 11/780 series computer were used.

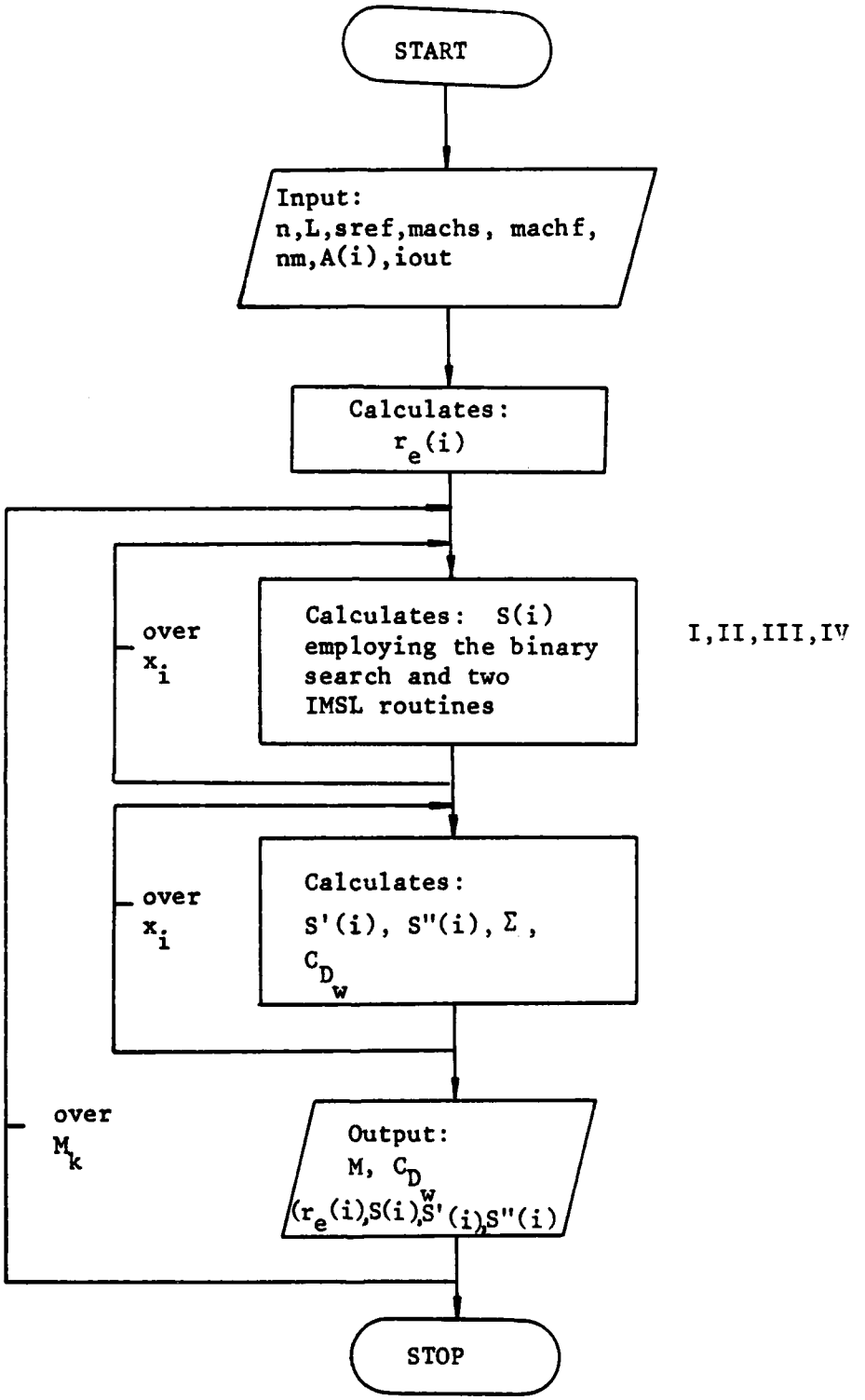

Figure 26. Flow Chart of the New Proposed Simplifications

Once the necessary input data were entered an equivalent body of revolution was constructed, i.e., the equivalent body radii re(i) i = 1,2,. . .,n, were calculated by equating the aircraft cross-sectional area at a given longitudinal location x to a circle that represented the equivalent body of revolution cross-section at the same x using in both cases the same planes normal to the x - axis. Having that the following step was performed in 2-D space: the Mach cone started to move from $x_1 = \Delta x$ through the location given by $x_{n-1} = (n-1)\Delta x$ (for Versions I and II) or to $x_n = n\Delta x$ (for Versions III and IV). At every x_m an area S_m was obtained in one among the four ways described in Section 2 - Four New Proposed Simplifications of the Supersonic Area Rule. It was necessary to employ a searching routine and another routine for approximation. The binary search technique and two IMSL routines (ICSCCU and ICSEVU) were employed. (The ICSCCU routine calculated elements of the cubic spline matrix which were needed for the ICSEVU routine to calculate re(x) at any given x between x_1 and $x_n = L$.) The way in which the searching routine employed works can be easily seen from Figure 27 and will be discussed later. By using either between the Mach cone generators in the xOz- plane and the equivalent body of revolution contour, intersection points were found. Once the intersection point was found, i.e., x = t was known and re(t) easily calculated, it was simple to calculate the area according to any approach among the four described. (When either Version III or IV is to be used the user needs to include the point 0(0,0) in calculations. Otherwise, the IMSL routines are required to calculate re at an $x < x_1$, i.e., outside the interval given as (x_1,L), and the rest of the computation gives wrong results.)

Calculation of S(i) was performed at every axial location within a do-loop over "i" (Figure 26). Once all of the S(i) were found, a new equivalent body of revolution was constructed. That is, the body of revolution obtained for a given Mach number of interest from the initial body of revolution (that one which the whole aircraft structure was collapsed to). To apply Eq (21) to that body, the second derivative S"(x) was needed. From numerical analysis it is known that none of the procedures for finding derivatives numerically is reliable enough -- even finding the first derivative numerically can give results which are too far from exact values. The reason for this situation is that two functions can be very close to each other as values of the functions are concerned, yet very different as for their slopes -- let aside the second derivatives. The following schemes were tried:

1. The cubic spline first and second derivative evaluator. There were oscillations in the second derivative sign due to the nature of the approximation by the cubic splines. Large errors occurred as a final result from this scheme.

2. Smoothing data and then applying the cubic splines. Then problems with the interval ends occurred.

3. The Newton forward and backward interpolation and then differentiation.

4. The Newton forward at the beginning of the interval, the Stirling formula in the middle, and the Newton backward formula at the end of the interval.

5. Divided differences and averaged slopes.

The last three procedures gave better results but still erroneous ones.

6. The scheme used in reference 3 which gave good results. (Along the way the scheme was slightly modified which resulted in a reduction of computation time of about 30 seconds for one Mach number.)

Having the second derivatives, the summation required was performed and the wave drag coefficient was calculated. The summation was broken into two parts and an analytical expression used to avoid singularity in the natural logarithm value as i = j, in the way described in reference 3. Then the procedure is repeated for another Mach number, i.e., a do-loop over Mach number was formed.

The following is a brief description of the binary searching routine as mentioned earlier.

The binary search procedure is known as a fast converging procedure for determining points of intersection between curves of different types. The reason for its fast convergence lies in starting the search by large steps and decreasing the step size by dividing it by two as the search comes closer to the point searched for. In this particular case, the Mach cone generator (ray), i.e., the Mach line, originated at x(i) will intersect the equivalent body contour re = re(x) at some point T, the abscissa of which is x = t (Figure 27a). The end points of the interval become the left (x_l) and right (x_r) limits. The first value of x at which the equivalent body radius will be found is determined by line #4 (Figure 27b). At that particular x = t a value for re is found by using the IMSL routines for the cubic spline interpolation -- lines #1 and #7. That is value r. If the r is close enough (within required accuracy) to the h-leg of the triangle, the search will stop and an area of interest will be found -- according to the program version employed (in Figure 27

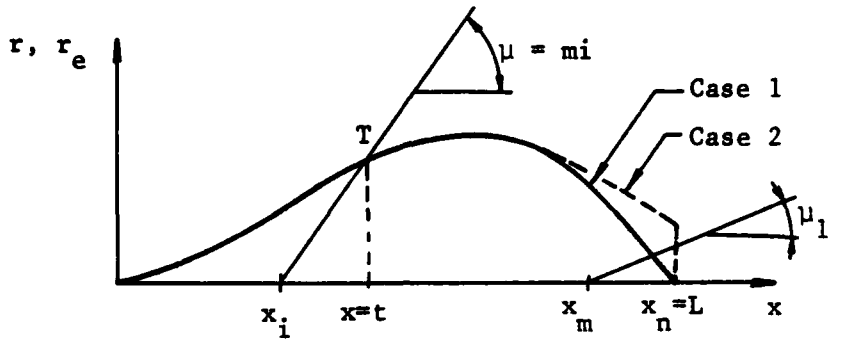

(a)

```
 1          call icsccu (x,re,n,c,200,ier)
 2          xl = x(i)
 3          xr = 1
 4    600   t = (xl + xr)/0.2d + 01
 5          h = (t - x(i)) * tan(mi)
 6          if( (1-t).lt.0.1d-02) go to 400
 7          call icsevu (x,re,n,c,t,r,1,ier)
 8          if (abs(h-r).lt.0.1d-02) go to 400
 9          if (h.lt.r) go to 500
10          xr = t
11          go to 600
12    500   xl = t
13          to to 600
14    400   S(i) = pi*h**2
```

(b)

Figure 27. Binary Search Procedure

it was Version II). After this, the originating point of the Mach cone generator was moved along the x - axis for the step size Δx, and a new searching cycle was performed. Line #6 becomes prominent when $A(L) \neq 0$, and $h < re(L)$, case 2 in Figure 27a.

```
c     ************************************************************
c     *                                                          *
c     *          P R O G R A M      C D W 2 . F                  *
c     *                                                          *
c     ************************************************************
c
c
c     This program calculates the wave drag coefficient,
c     by employing a modification to the standard supersonic
c     area rule as proposed by Capt. First Class Vojin R. Nikolic
c     - Yugoslav Air Force. The program was written as a part of
c     his thesis project ; 1983.
c
c     The input data set required consists of:
c         n = the number of steps along the aircraft longitudinal
c             axis; recommended n = 100 to 200.
c         l = the aircraft length
c         sref = reference area
c         machs = the lowest Mach number at which the wave drag
c                 is to be calculated
c         machf = the highest Mach number at which the wave drag
c                 is to be calculated
c         nm = the number of Mach number steps
c         iout = the integer which determines the form in which
c                the output will appear in the following manner:
c                if iout = 1 the results will appear as a table
c                            consisting of the Mach numbers and
c                            the wave drag coefficient values
c                if iout = 2 the output will include results of
c                            following intermediate steps:
c                            - equivalent body of revolution
c                              radii,
c                            - Mach cone cut area distributions,
c                            - First and second derivative of
c                              the area distributions,
c                            The above three groups of results
c                            will be given at every x(i) -
c                            axial location
c         a(i) = the cross-sectional areas at n locations
c
      common a(200),re(200),s(200),x(200),c(200,3),y(200),sx(200),
     1unky(400),ap(205)
      real machs,machf
      integer n,ier
```

```
      double precision x(200),re(200),s(200),t,r,l,mach,mi,dx,
     1c(200,3)
      open(7,file='inpcdw')
      rewind 7
      open(6,file='outcdw')
      rewind 6
c
c     This part of the program reads the set of input data. The
c     double precision formats are necessary if IMSL routines
c     are to be used on the VAX 11/780 series computer.
c
      read (7,10) n
10    format(i4)
      read (7,11) l
11    format(d12.5)
      read (7,12) sref
12    format(f8.3)
      read (7,11) machs
      read (7,11) machf
      read (7,15) nm
15    format(i2)
      read(7,17) iout
17    format(i1)
c
c     The following part of the program writes the input set
c     except for the a(i) values forming a heading of the
c     output.
c
      write (6,20) n,l,sref,machs,machf,nm,iout
20    format(10(/),15x,'INPUT DATA',/,37x,
     1'for the wave drag coefficient (Cdw) calculation',//,38x,
     2'Number of steps along the x-axis : n =',1x,i4,/,
     338x,'Length : l =',1x,f8.3,1x,'ft',/,38x,
     4'Referent area : sref =',1x,f8.3,1x,'sq ft',/,38x,
     5'Free stream Mach numbers are :',/,40x,
     6'- Mach number to start with : machs =',1x,f4.2,/,40x,
     7'- Mach number to finish with : machf =',1x,f4.2,/,40x,
     8'- Number of Mach number steps : nm =',1x,i2,//,38x,
     9'Output will appear in form :',1x,i1)
c
      pi=0.31415926536d+01
      dx=1/n
c
      if(iout.eq.2) write(6,30)
c
c     Now the cross-sectional areas are read in and radii
```

```
c       of an equivalent body of revolution are calculated.
c
        do 100 i=1,n
        read (7,40) a(i)
40      format(f12.5)
        x(i)=i*dx
        re(i)=sqrt(a(i)/pi)
        if(iout.eq.2) write(6,50) i,x(i),a(i),re(i)
100     continue
c
c       The IMSL routine ICSCCU calculates the cubic spline
c       coefficient matrix, C.
c
        call icsccu (x,re,n,c,200,ier)
        fnm=float(nm)
        dmach=(machf-machs)/fnm
        mach=machs-dmach
        if(iout.eq.1) write(6,21)
c
c       Now the outer do loop within the program - that
c       one over Mach numbers starts.
c
        do 800 K=1,nm+1
        mach=mach+dmach
        mi=asin(0.1d+01/mach)
c
c       Do loop 700 does the following:
c                   - finds the intersection points
c                     between the Mach lines and the
c                     equivalent body of revolution
c                     contour, (the binary search and
c                     the IMSL routines ICSCCU and
c                     ICSEVU are used)
c                   - calculates the forward projections
c                     of the Mach cone cut areas (label
c                     400)
c
        do 700 i=1,n-1
        xl=x(i)
        xr=1
600     t=(xl+xr)/0.2d+01
        h=(t-x(i))*tan(mi)
        if((1-t).lt.0.1d-02) go to 400
        call icsevu (x,re,n,c,200,t,r,1,ier)
        if(abs(h-r).lt.0.1d-02) go to 400
        if(h.lt.r) go to 500
```

```
        xr=t
        go to 600
500     xl=t
        go to 600
400     s(i)=pi*h**2
700     continue
c       connection
c       conversion : double precision into single precision
        nxy=n-1
        do 711 i=1,n-1
        y(i)=sngl(s(i))
        sx(i)=sngl(x(i))
711     continue
        el=sngl(l)
c
c       The first derivatives of the area distributions
c       S(x) - using a nested average technique, (up to label 23)
c
        unky(101)=y(2)/(2.*dx)
        unky(100+nxy)=(y(nxy)-y(nxy-1))/dx
        unky(99+nxy)=(y(nxy)-y(nxy-2))/(2.*dx)
        do 23 j=3,nxy-1
        tri=(y(j)-y(j-2))/(2.*dx)
        quad1=(y(j+1)-y(j-2))/(3.*dx)
        if(j.eq.3) then
        quad2=y(j)/(3.*dx)
        pent=y(j+1)/(4.*dx)
        else
        quad2=(y(j)-y(j-3))/(3.*dx)
        pent=(y(j+1)-y(j-3))/(4.*dx)
        end if
        quad=(quad1+quad2)/2.
        unky(99+j)=(tri+quad+pent)/3.
23      continue
c
c       The second derivative of the area distribution S"(x)
c       using the same technique as above , (up to label 25)
c
        ap(1)=0.0
        ap(2)=(unky(102))/(2.*dx)
        ap(nxy+1)=(unky(100+nxy)-unky(99+nxy))/dx
        ap(nxy)=(unky(100+nxy)-unky(98+nxy))/(2.*dx)
        do 25 j=2,nxy-2
        tri=(unky(j+101)-unky(j+99))/(2.*dx)
        quad1=(unky(j+102)-unky(j+99))/(3.*dx)
        if(j.eq.2) then
```

AD-A137 018 AN INVESTIGATION OF NEW POSSIBILITIES TO SIMPLIFY THE STANDARD SUPERSONIC AREA RULE(U) AIR FORCE INST OF TECH WRIGHT-PATTERSON AFB OH SCHOOL OF ENGI.. V R NIKOLIC

2/2

UNCLASSIFIED DEC 83 AFIT/GAE/AA/83D-16 F/G 20/4 NL

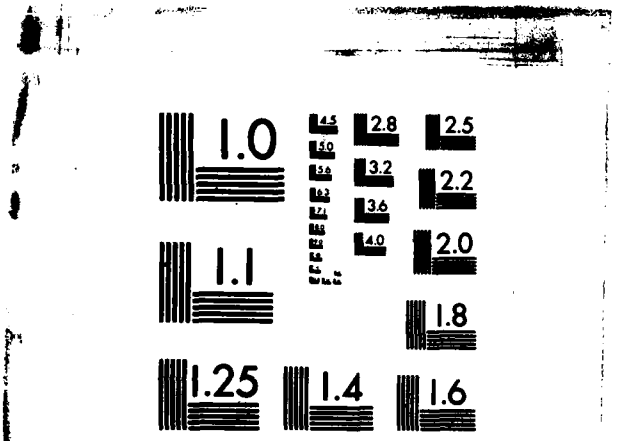

```
      quad2=(unky(j+101))/(3.*dx)
      pent=(unky(j+102))/(4.*dx)
      else
      quad2=(unky(j+101)-unky(j+98))/(3.*dx)
      pent=(unky(j+102)-unky(j+98))/(4.*dx)
      end if
      quad=(quad1+quad2)/2.
      ap(j+1)=(tri+quad+pent)/3.
25    continue
c
c     Now the numerical integration needed is performed
c     and the wave drag coefficient is calculated.
c     Then the results are written in the form
c     determined by the iout value.
c
      cdwtot=0.0
      wdtot=0.0
      cwdtot=0.0
      do 27 i=1,nxy
      cdwtot=0.0
      do 26 j=1,nxy
      xi=i
      xj=j
      xnxy=nxy
      argu=(xi/xnxy-(xj-1.)/xnxy)
      arg=abs(xi/xnxy-xj/xnxy)
      if(j.lt.i.or.j.gt.i) cdw=ap(j)*alog(arg)*el/nxy
      if(j.eq.i) cdw=ap(j)*2.*(el*(-abs(argu*alog(argu)-argu)))
      cdwtot=cdwtot+cdw
26    continue
      wdtot=ap(i)*el/nxy*cdwtot
      cwdtot=cwdtot+wdtot
27    continue
      cdwtot=-.5*cwdtot/3.1415927/sref
      cdw=cdwtot/2.
      if(iout.eq.1) then
21    format(6(/),60x,'RESULTS',/,60x,7('='),//,
     137x,53('-'),/,37x,'I',25x,'I',25x,'I',/,
     237x,'I',12x,'M',12x,'I',11x,'CDw',11x,'I',/,
     337x,'I',25x,'I',25x,'I',/,37x,53('-'))
      write(6,31) mach,cdw
31    format(37x,'I',10x,f4.2,11x,'I',9x,f7.5,
     19x,'I',/,37x,53('-'))
      else
30    format(///,48x,'EQUIVALENT BODY OF REVOLUTION RADII',
     1///,49x,'i',9x,'x(i)',11x,'a(i)',8x,'re(i)',/)
```

```
50      format(/,46x,i4,4x,d12.5,4x,f8.3,4x,a12.5)
        write(6,60) mach
60      format(4(/),50x,'MACH CONE CUT AREA DISTRIBUTION',/,63x,
     1'M =',1x,f4.2,//,50x,'i',9x,'x(i)',15x,'s(x)',/)
        do 701 i=1,n-1
        write(6,70) i,x(i),s(i)
70      format(/,48x,i3,3x,d12.5,8x,d12.5)
701     continue
        write(6,80) mach
80      format(////,47x,'FIRST AND SECOND DERIVATIVE OF S(X)',/,
     160x,'M =',1x,f4.2,//,32x,'i',10x,'x(i)',11x,
     2'fder(i)',9x,'sder(i)',13x,'s(x)',//)
        do 704 i=1,nxy
        write(6,81) i,sx(i),unky(100+i),ap(i+1),y(i)
81      format(/,30x,i3,4x,f12.7,4x,f12.7,4x,f12.7,4x,f12.7)
704     continue
        write(6,28)mach,cdw
28      format(//,'At a Mach number of :',1x, f4.2,
     12x,'the wave drag coefficient is :',f7.5)
        end if
800     continue
        end
%
```

Vita

Vojin Rade Nikolic was born on November 10, 1950 in Decane, Yugoslavia. He graduated from high school in Titograd, Yugoslavia in 1969. In 1972 he joined the Yugoslav Air Force. From 1975 to 1978 he attended the University of Belgrade, Belgrade, Yugoslavia, where he earned the degree of Bachelor of Science in Aerospace Engineering. In June 1982 he entered the School of Engineering, Air Force Institute of Technology.

UNCLASSIFIED

SECURITY CLASSIFICATION OF THIS PAGE

REPORT DOCUMENTATION PAGE

1a. REPORT SECURITY CLASSIFICATION: UNCLASSIFIED	1b. RESTRICTIVE MARKINGS
2a. SECURITY CLASSIFICATION AUTHORITY	3. DISTRIBUTION/AVAILABILITY OF REPORT: Approved for public release; distribution unlimited.
2b. DECLASSIFICATION/DOWNGRADING SCHEDULE	
4. PERFORMING ORGANIZATION REPORT NUMBER(S): AFIT/GAE/AA/83D-16	5. MONITORING ORGANIZATION REPORT NUMBER(S)
6a. NAME OF PERFORMING ORGANIZATION: School of Engineering; 6b. OFFICE SYMBOL (If applicable): AFIT/ENY	7a. NAME OF MONITORING ORGANIZATION
6c. ADDRESS (City, State and ZIP Code): Air Force Institute of Technology, Wright-Patterson AFB, Ohio 45433	7b. ADDRESS (City, State and ZIP Code)
8a. NAME OF FUNDING/SPONSORING ORGANIZATION; 8b. OFFICE SYMBOL (If applicable)	9. PROCUREMENT INSTRUMENT IDENTIFICATION NUMBER
8c. ADDRESS (City, State and ZIP Code)	10. SOURCE OF FUNDING NOS. — PROGRAM ELEMENT NO. / PROJECT NO. / TASK NO. / WORK UNIT NO.
11. TITLE (Include Security Classification)	
12. PERSONAL AUTHOR(S): Vojin R. Nikolic, Capt. 1st Class, YAF	
13a. TYPE OF REPORT: MS Thesis; 13b. TIME COVERED: FROM _____ TO _____	14. DATE OF REPORT (Yr., Mo., Day): 1983 December; 15. PAGE COUNT: 90
16. SUPPLEMENTARY NOTATION	Approved for public release: IAW AFR 190-17. LYNN E. WOLAVER, Dean for Research and Professional Development, Air Force Institute of Technology (ATC), 3 JAN 1984

17. COSATI CODES		
FIELD	GROUP	SUB. GR.
20	04	

18. SUBJECT TERMS (Continue on reverse if necessary and identify by block number): Supersonic Aircraft Configurations, Wave Drag, Supersonic Area Rule, Simplified Supersonic Area Rule

19. ABSTRACT (Continue on reverse if necessary and identify by block number)

Title: AN INVESTIGATION OF NEW POSSIBILITIES TO SIMPLIFY THE STANDARD SUPERSONIC AREA RULE

Thesis Chairman: Eric J. Jumper, Major, USAF

20. DISTRIBUTION/AVAILABILITY OF ABSTRACT: UNCLASSIFIED/UNLIMITED ☒ SAME AS RPT. ☐ DTIC USERS ☐	21. ABSTRACT SECURITY CLASSIFICATION: UNCLASSIFIED

22a. NAME OF RESPONSIBLE INDIVIDUAL	22b. TELEPHONE NUMBER (Include Area Code)	22c. OFFICE SYMBOL
Eric J. Jumper, Major, USAF	513-255-3517	AFIT/ENY

DD FORM 1473, 83 APR — EDITION OF 1 JAN 73 IS OBSOLETE.

UNCLASSIFIED

SECURITY CLASSIFICATION OF THIS PAGE

A modified method of the supersonic-area-rule-type was developed. Instead of using the axis normal projection of the area cut by the oblique Mach planes through the full aircraft configuration suggested by Jones, Lomax, and Whitcomb, the down-stream Mach cone lateral surface was used on the equivalent body of revolution of the configuration. A computer program to perform the required calculations according to this modified procedure was written. Several cases of actual aircraft configurations and wind tunnel models were used for numerical investigation of the method. Some promising results were found along with tremendous decreases in both core storage and computing time required by the full supersonic area rule.

END

FILMED

2-84

DTIC